Selective G-quadruplex binding by oligoarginine-Ru(dppz) metallopeptides

David Bouzada, Iria Salvadó, Ghofrane Barka, Gustavo Rama, José Martínez-Costas, Romina Lorca, Álvaro Somoza, Manuel Melle-Franco, M. Eugenio Vázquez and Miguel Vázquez López*

Electronic Supporting Information (ESI)

General

All reagents were acquired from commercial sources: Dimethyl sulfoxide (DMSO), Dimethylformamide (DMF) and Trifluoroacetic acid (TFA) were purchased from Scharlau, EtOH and CH_2Cl_2 from Panreac and CH_3CN from Merck. All peptide synthesis reagents, namely the coupling agents HBTU (O-Benzotriazole-N,N,N',N'-tetramethyl-uronium-hexafluorophosphate) and HATU (2-(1H-7-azabenzotriazol-1-yl)-1,1,3,3-tetramethyluronium hexafluorophosphate methanaminium), and Fmoc amino acid derivatives were purchased from GL Biochem (Shanghai) Ltd. Fmoc-Rink amide AM resin was purchased from Iris Biotech. The oligonucleotides were purchased from Thermo Fisher Scientific GmbH. All other chemicals were purchased from Alfa-Aesar, Sigma-Aldrich or Fluka. All solvents were dry and of synthesis grade, unless specifically noted. $RuCl_3.3H_2O$ was purchased from Matthews Chemicals. Reactions were followed by analytical RP-HPLC with an Agilent 1100 series LC/MS using a Luna C18 (250 x 4.60 mm) analytical column from Phenomenex. Standard conditions for analytical RP-HPLC consisted on a linear gradient from 30% to 95% of solvent B for 30 min at a flow rate of 1 mL/min (A: water with 0.1% TFA, B: acetonitrile with 0.1% TFA). Compounds were detected by UV absorption at 222, 254 and 310 nm. High-Performance Liquid Chromatography (HPLC) was performed using an Agilent 1100 series Liquid Chromatograph Mass Spectrometer system. Analytical HPLC was run using a Luna C18 (250 x 4.60 mm) reverse phase analytical column; compounds were detected by UV absorption at 222, 254 and 310 nm. The purification of the peptides was performed on a Luna C18 (250 x 10 mm) semi-preparative reverse phase column from Phenomenex. The standard gradient used for analytical and semi-preparative HPLC was 70:30 to 5:95 over 30 min (water/acetonitrile, 0.1% TFA). Compounds were detected by UV absorption (222 nm) and by ESI^+−MS. The fractions containing the products were freeze-dried, and their identity was confirmed by ESI^+−MS and MALDI-TOF. Electrospray Ionization Mass Spectrometry (ESI/MS) was performed with an Agilent 1100 Series LC/MS model in positive scan mode using direct injection of the purified peptide solution into the MS. Matrix-assisted laser desorption/ionization mass spectrometry (MALDI/MS) was performed with a Bruker Autoflex MALDI/TOF model in positive scan mode by direct irradiation of the matrix-absorbed peptide. Luminescence experiments were made with a Jobin-Yvon Fluoromax-3 fluorescence spectrometers (DataMax 2.20), coupled to a Wavelength Electronics LFI−3751 temperature controller. All measurements were made with a Hellma semi-micro cuvette (114F-QS) at 20 ºC. CD experiments were made with a *Jasco J-715* coupled to a *Neslab RTE-111* thermostarted water bath at 20ºC. UV-vis absorption experiments were performed in a *Jasco V-630* spectrophotometer coupled to a *Jasco ETC-717* temperature controller at 20ºC.

Synthesis of the unnatural coordinating residue Fmoc-βAla-bpy-OH (1)

The coordinating residue Fmoc-βAla-bpy-OH (1) was synthesized following a procedure previously reported by our research group. [1]

Synthesis of the peptide ligands

C-terminal amide peptides were synthesized by following standard SPPS protocols on a 0.1 mmol scale using a 0.45 mmol/g Fmoc-Rink-amide resin. Arginines were coupled, in 10-fold excess (vs. mmol of resin load), by using *O*-(benzotriazol-1-yl)-*N,N,N',N'*-tetramethyluronium hexafluorophosphate (HBTU) as an activating agent.

Fmoc-βAlaBpy-OH (**1**) was coupled in 5-fold excess using O-(7-Azabenzotriazol-1-yl)-*N,N,N',N'*-tetramethyluronium hexafluorophosphate (HATU) as activating agent.

Couplings were conducted for 1 h. Deprotection of the temporal Fmoc protecting-group was performed with 20% piperidine in DMF for 15 min.

Test cleavages were performed at a 1 mg scale for 2 h with CH_2Cl_2 (50 μL), H_2O (25 μL), TIS (triisopropylsilane, 25 μL), and TFA (900 μL) (~1 mL of cocktail for 20 mg of resin).

Synthesis of the Ru(II) metallopeptides

Common step

Once the peptide ligand were synthesized, 222 mg of the resin with the corresponding peptide anchored was suspended in 3 mL of EtOH:DMF (1:1) in the dark and the resulting mixture were purged with Ar for 15 min. 54.6 mg (1.3 eq) of $[Ru(DMSO)_4Cl_2]$[16] was added and the resulting mixture was stirred under argon for 24 hours at 80 ºC. Then, the resin was washed with DMF (5 x 10 mL, 10 min) and dried under vacuum.

[Ru(dppz)] and [Ru(dppz)]-R_8

The resin was then suspended in 3 mL of EtOH:DMF (1:1) in the dark and the resulting mixture were purged with Ar for 15 min. 18.0 mg (1.0 eq) of 1,10'-phenantroline was added and the resulting mixture was stirred under argon for 24 hours at 80 ºC. Then, the resin was washed with DMF (5 x 10 mL, 10 min) and dried under vacuum.

Finally, the resin was suspended in 3 mL of EtOH:DMF (1:1) in the dark and the resulting mixture were purged with Ar for 15 min. 28.2 mg (1.0 eq) of dipyrido[3,2-a:2',3'-c]phenazine (dppz)[17] was added and the resulting mixture was stirred under argon for 24 hours at 80 ºC. Then, the resin was washed with DMF (5 x 10 mL, 10 min) and dried under vacuum.

[Ru(dppz)$_2$] and [Ru(dppz)$_2$]-R_8

The resin was then suspended in 3 mL of EtOH:DMF (1:1) in the dark and the resulting mixture were purged with Ar for 15 min. 56.5 mg (2.0 eq) of dipyrido[3,2-a:2',3'-c]phenazine (dppz)[17] was added and the resulting mixture was stirred under argon for 24 hours at 80 ºC. Then, the resin was washed with DMF (5 x 10 mL, 10 min) and dried under vacuum.

General procedure for peptide cleavage-deprotection

The resin was filtered, washed with DMF and CH_2Cl_2 and dried. The metallopeptide was cleaved with 5 mL of the standard TFA cocktail (TIS, H_2O, CH_2Cl_2 and TFA) over 2.5 hours. After that, the resin was filtered and washed with TFA (1 x 2 mL) and the filtrate was concentrated until 1 mL of volume

with a N_2 stream. Then, 4 mL of H_2O and 5 mg of NH_4PF_6 were added to this solution. The red orange solid precipitated was separated by centrifugation, washed with H_2O (1 x 4 mL) and purified by semi-preparative HPLC to give the desired product.

[Ru(DMSO)Cl_2] and dipyrido[3,2-a:2',3'-c]phenazine (dppz) were synthesized following reported procedures. [2,3]

Mass spectra and HPLC chromatograms of the Ru(II) metallopeptides

a) [Ru(dppz)]

MALDI-TOF: m/z calculated for $C_{43}H_{35}N_{11}O_3Ru$: 891.2, found: 890.2

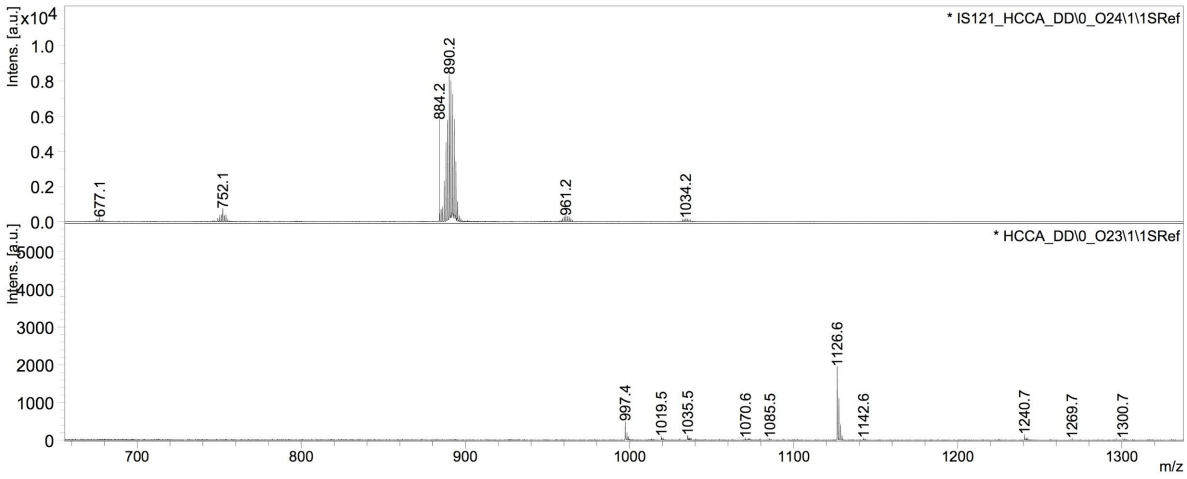

HPLC chromatogram: 1-75 %B, t_R=24.3´

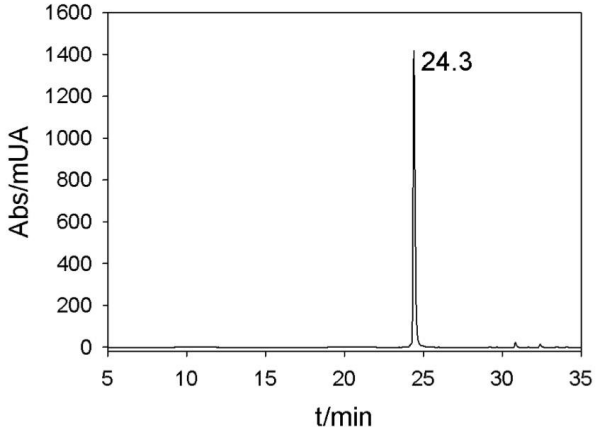

b) [Ru(dppz)]-R_8

MALDI-TOF: m/z calculated for $C_{94}H_{131}N_{43}O_{11}Ru$: 2140.0, found: 2141.1

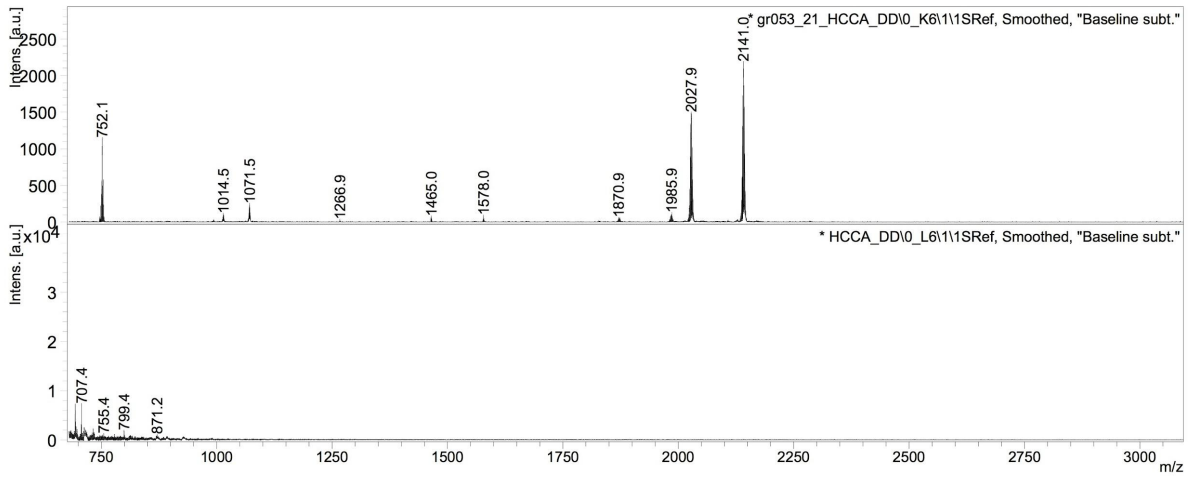

HPLC chromatogram: 1-75 %B, t_R=19.3'

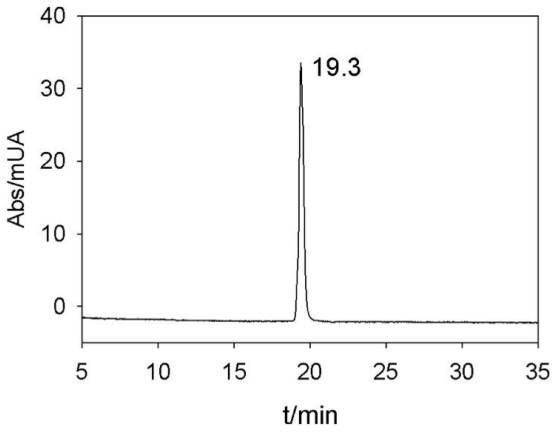

c)[Ru(dppz)$_2$]

MALDI-TOF: m/z calculated for $C_{52}H_{37}N_{13}O_3Ru$: 993.2, found: 993.2

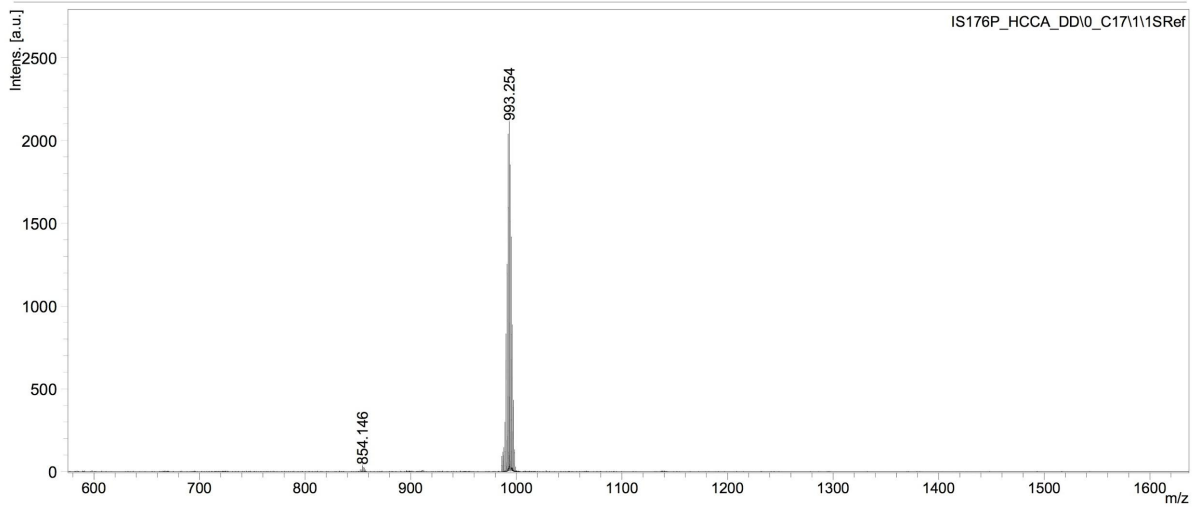

HPLC chromatogram: 1-75 %B, t_R=28.3´

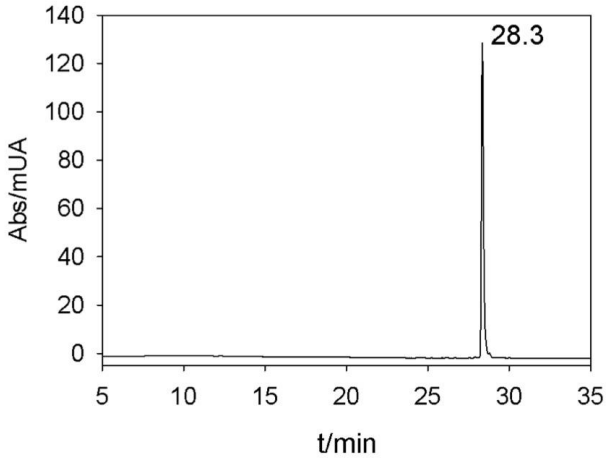

d) [Ru(dppz)$_2$]-R$_8$

MALDI-TOF: m/z calculated for $C_{100}H_{133}N_{45}O_{11}Ru$: 2242.0, found: 2244.0

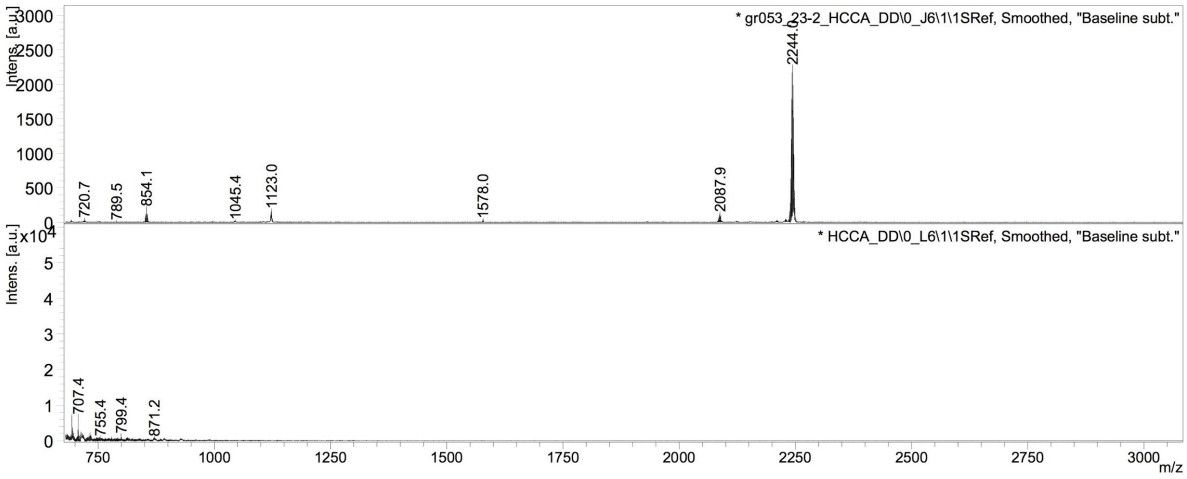

HPLC chromatogram: 1-75 %B, t_R=21.6

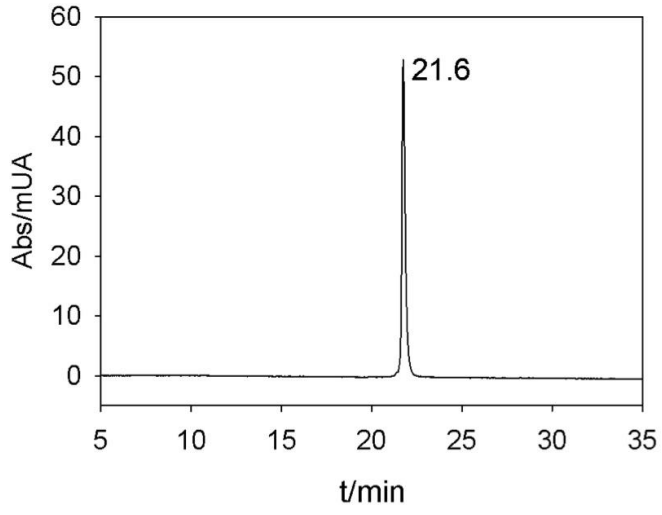

Fluorescence studies

DynaFit titration analysis

Experimental data were fitted with the *DynaFit 4.0* software, which performs a numerical treatment of the system. The program is available free of charge for academia at *http://www.biokin.com/dynafit/*

The program requires plain text files called *scripts* that contains information about the chemical model underlying the experimental data, the values of model parameters, such as starting concentrations of reactants, as well as information about location of the files. A typical script used in the analysis titrations is included below. The file has been commented to indicate the purpose of the keywords and sections.

```
[task]            ;semicolons indicate comments not read by the program
 task = fit       ;nature of the calculation to be performed by DynaFit
 data = equilibria

[mechanism]       ;This is a simple 1:1 binding model
 R + L <==> RL : Kd dissoc    ;indicates that it's a dissociation constant

[constants]       ;Initial Kd value for iteration
 Kd = 1.0 ?       ;the "?" indicates that this will be optimized

[concentrations]
 R = 2.0          ;Fixed concentration of the Ruthenium complexes

[responses]       ;contribution to the spectroscopic signal
 R = 0.1 ?
 RL = 1.5 ?

[data]            ;location of files and information about the data
 variable  L      ;indicates the species that changes its concentration
 offset auto ?
 directory ./exp/EVS/KIT      ;path relative to DynaFit location
 extension txt
 file f1          ;name of the experimental data file

[output]
 directory ./exp/EVS/KIT/out ;path indicating location of files

 [settings]       ;cosmetic settings that control DynaFit graphics
 {Output}
 XAxisUnit = uM
 BlackBackground = n
 XAxisLabel = [L]
 YAxisLabel = Emission Intensity
 WriteTXT = y
```

a) B-DNA binding studies

To a 2.0 μM solution of the selected Ru(II) metallopeptide (**[Ru(dppz)]** and **[Ru(dppz)]-R_8**) in Tris.HCl buffer (20 mM), pH 7.5 and NaCl (100 mM), aliquots of the selected B-DNA (GAATTC) stock solution (in water) were added and the fluorescence spectrum was recorded after each addition. The additions were carried out until no further changes in the emission spectra were detected. The studied B-DNA oligonucleotide is listed in Table S1.

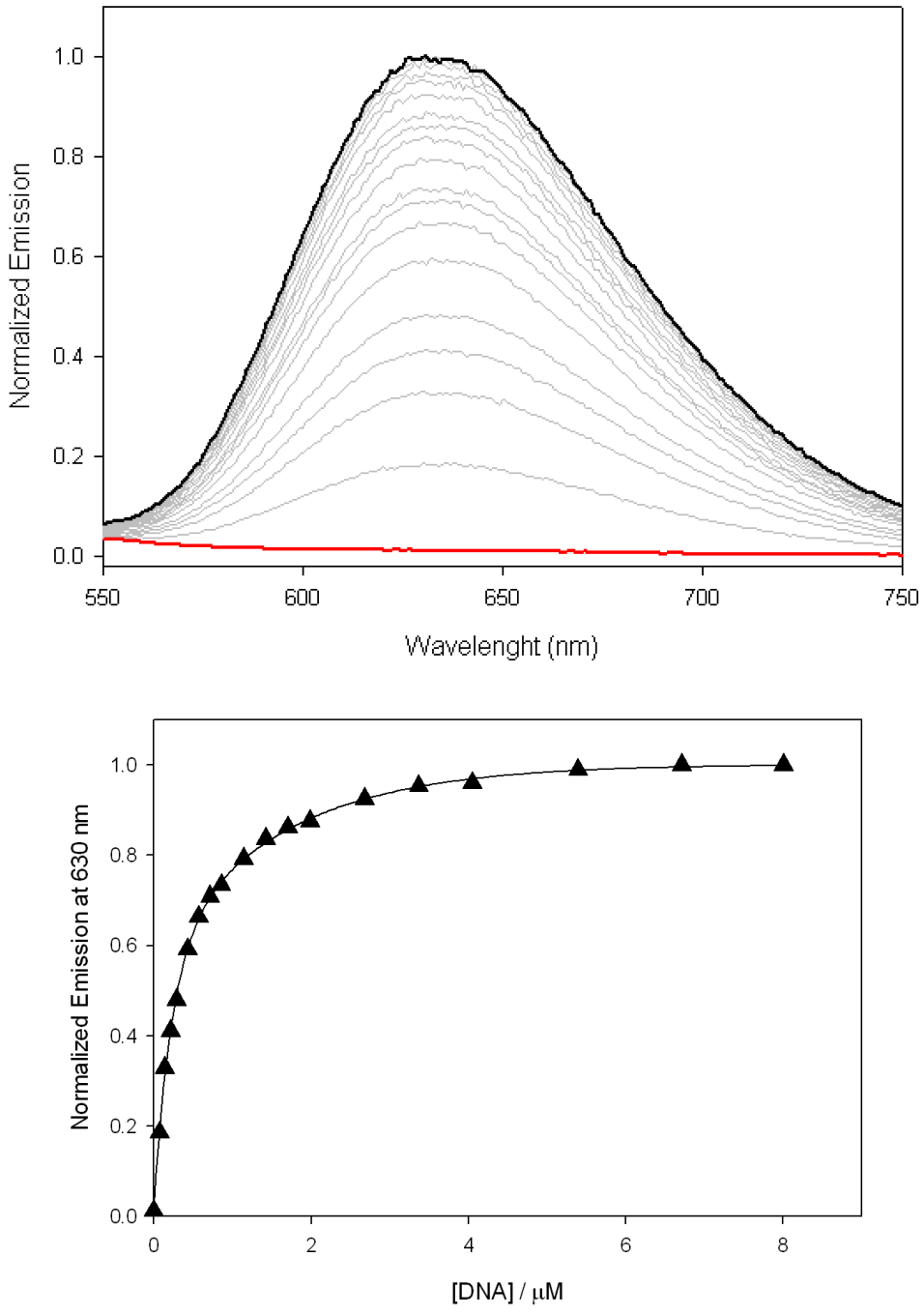

*Figure S1. Top, luminescence spectra of a 2.0 μM solution of **[Ru(dppz)]** in Tris-HCl buffer (20 mM), NaCl (100 mM), pH 7.5 and evolution upon addition of aliquots of GAATTC oligonucleotide solution until saturation; bottom, profile (black circles) of the fluorescence titration experiment of **[Ru(dppz)]** with GAATTC oligonucleotide at λ_{em} = 630 nm (emission intensity vs. concentration of DNA in the media) with the corresponding best fit (black line).*

In the case of the metallopeptide **[Ru(dppz)]** we were able to calculate the corresponding K_d, which has a value of 0.19 (0.03) μM, very similar to those reported in literature by similar complexes.[4] However, the profile of the titration experiment of **[Ru(dppz)]-R$_8$** at λ_{em} = *630 nm* indicate a two-step complex process which could be related to a very high affinity of this metallopeptide for the duplex DNA. As a consequence, it has not been possible to calculate the dissociation constant for this particular interaction. Further experiments will be needed in order to study conveniently this unusual behaviour.

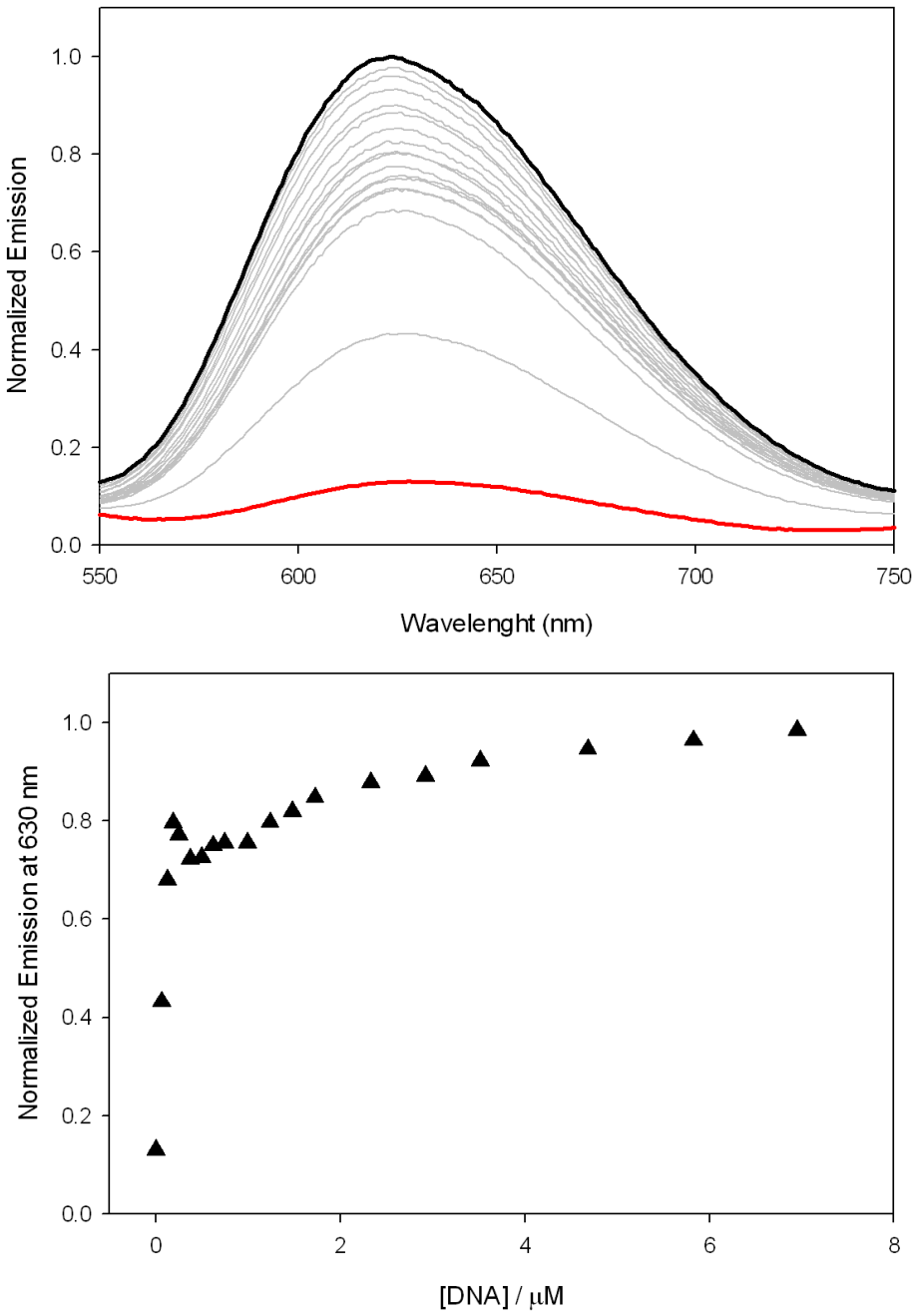

*Figure S2. Top, luminescence spectra of a 2.0 μM solution of **[Ru(dppz)]-R$_8$** in Tris-HCl buffer (20 mM), NaCl (100 mM), pH 7.5 and evolution upon addition of aliquots of GAATTC oligonucleotide solution until saturation; bottom, profile (black triangles) of the fluorescence titration experiment of **[Ru(dppz)]-R$_8$** with GAATTC oligonucleotide at λ_{em} = 630 nm (emission intensity vs. concentration of DNA in the media).*

b) G-quadruplex binding studies

To a 2.0 μM solution of the selected Ru(II) metallopeptide (**[Ru(dppz)]**, **[Ru(dppz)]-R_8**, **[Ru(dppz)$_2$]** and **[Ru(dppz)$_2$]-R_8**) in phosphate buffer (100 mM), pH 7.5 and KCl (1.0 M), aliquots of G-quadruplex stock solution (in water) were added and the fluorescence spectrum was recorded after each addition. The additions were carried out until no further changes in the emission spectra were detected. The studied oligonucleotides are listed in Table S1.

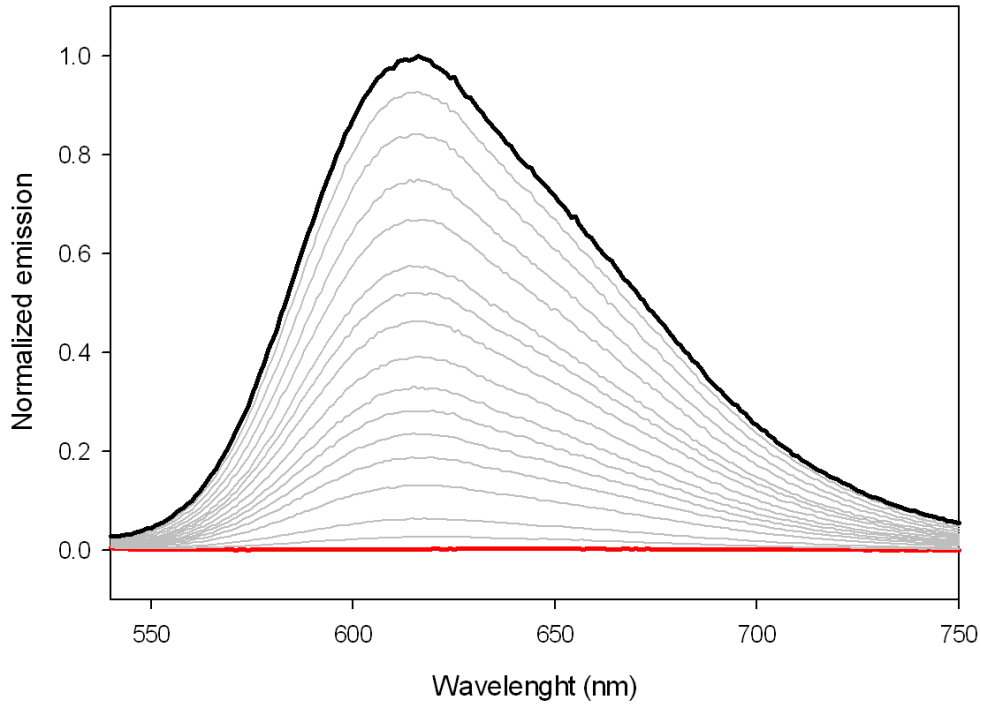

*Figure S3. Top, luminescence spectra of a 2.0 μM solution of **[Ru(dppz)]** in phosphate buffer (100 mM), KCl (1.0 M), pH 7.5 and evolution upon addition of aliquots of TEL oligonucleotide solution until saturation.*

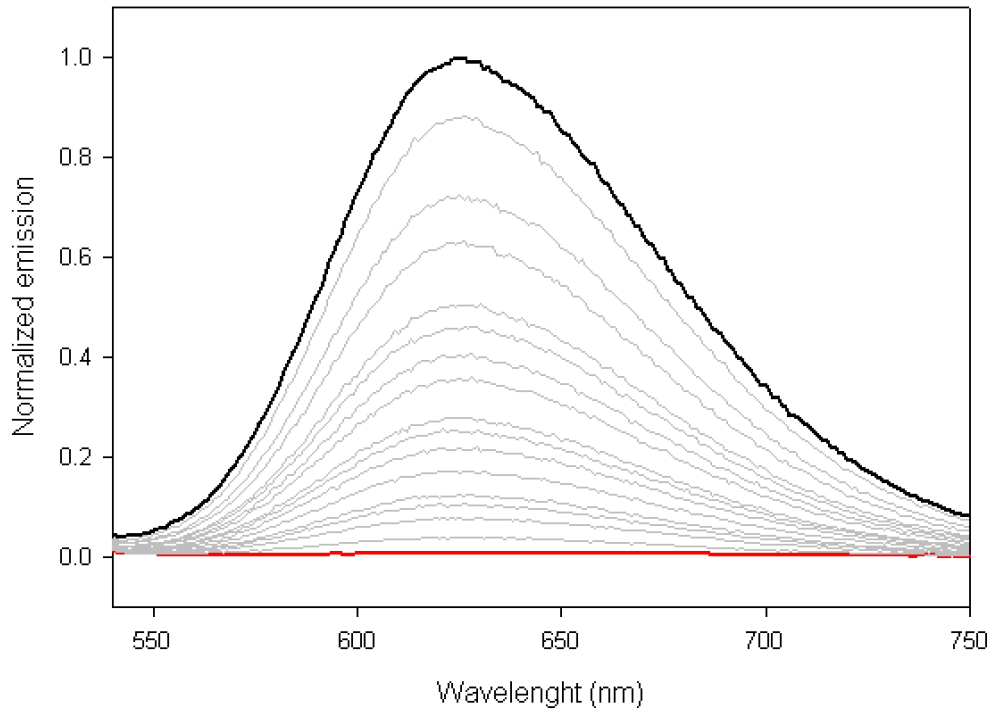

Figure S4. Top, luminescence spectra of a 2.0 μM solution of ***[Ru(dppz)]*** *in phosphate buffer (100 mM), KCl (1.0 M), pH 7.5 and evolution upon addition of aliquots of KIT oligonucleotide solution until saturation.*

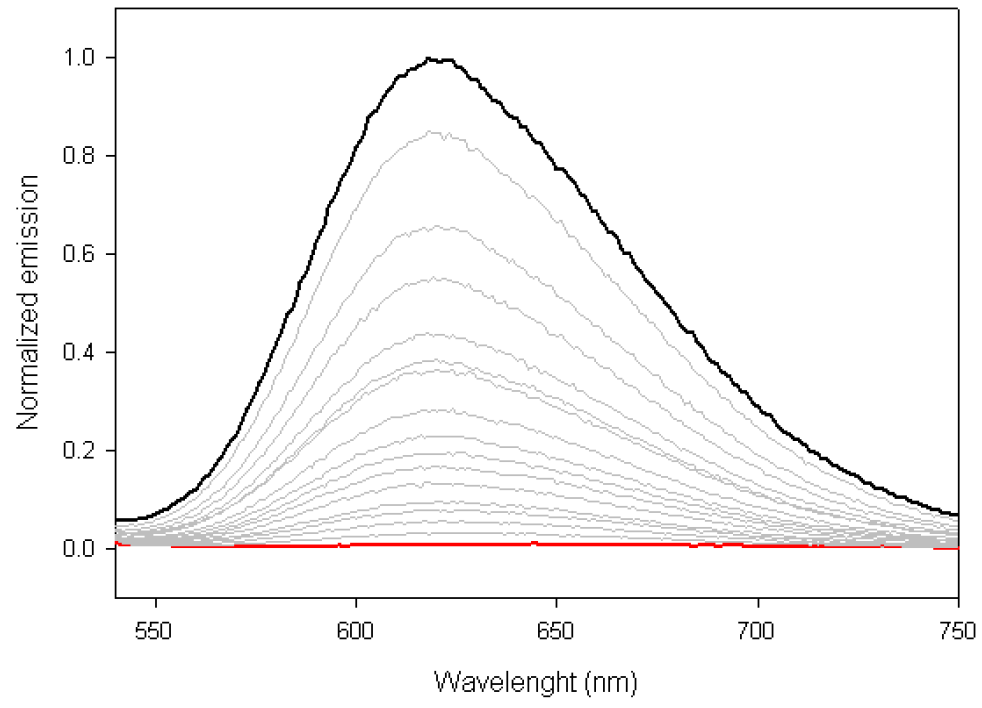

Figure S5. Top, luminescence spectra of a 2.0 μM solution of ***[Ru(dppz)]*** *in phosphate buffer (100 mM), KCl (1.0 M), pH 7.5 and evolution upon addition of aliquots of MYC oligonucleotide solution until saturation.*

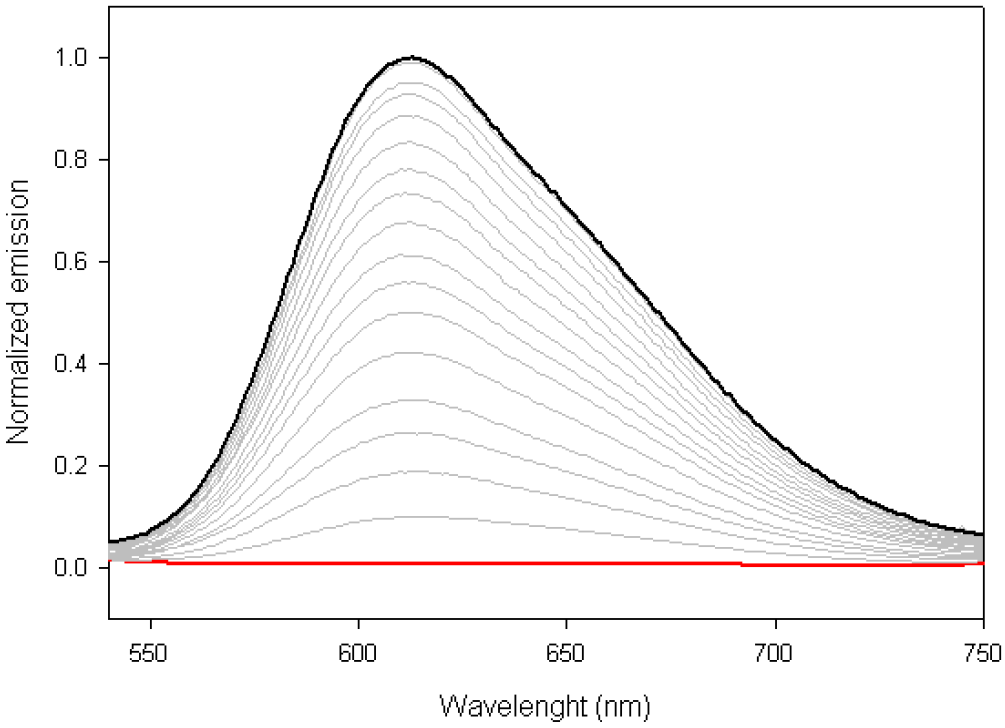

Figure S6. Top, luminescence spectra of a 2.0 μM solution of ***[Ru(dppz)]-R$_8$*** *in phosphate buffer (100 mM), KCl (1.0 M), pH 7.5 and evolution upon addition of aliquots of TEL oligonucleotide solution until saturation.*

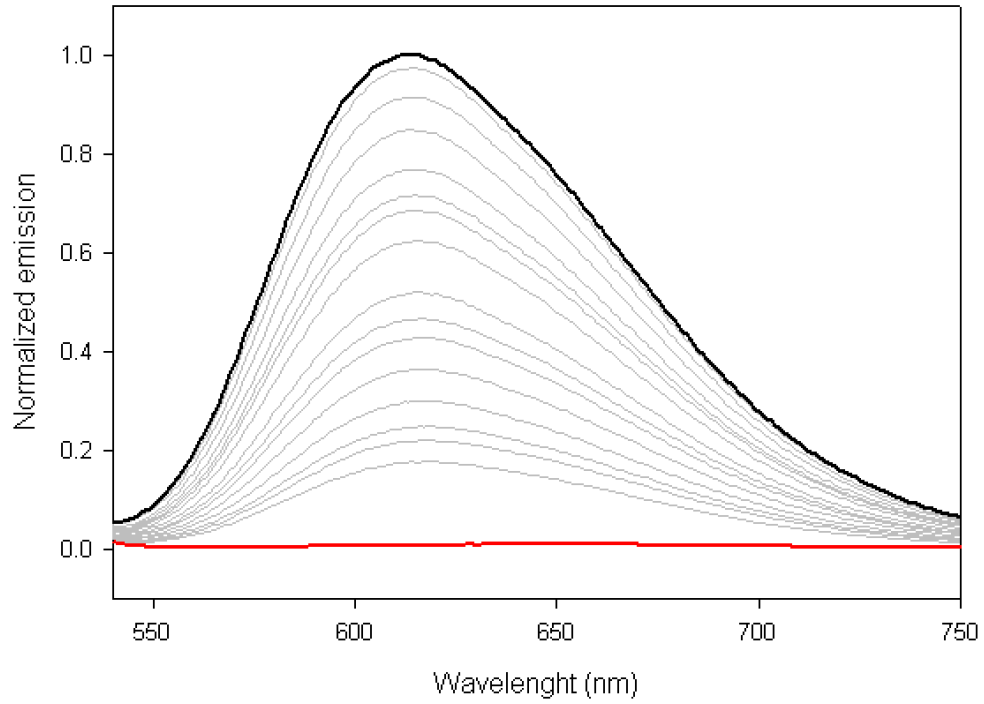

Figure S7. Top, luminescence spectra of a 2.0 μM solution of ***[Ru(dppz)]-R$_8$*** *in phosphate buffer (100 mM), KCl (1.0 M), pH 7.5 and evolution upon addition of aliquots of KIT oligonucleotide solution until saturation.*

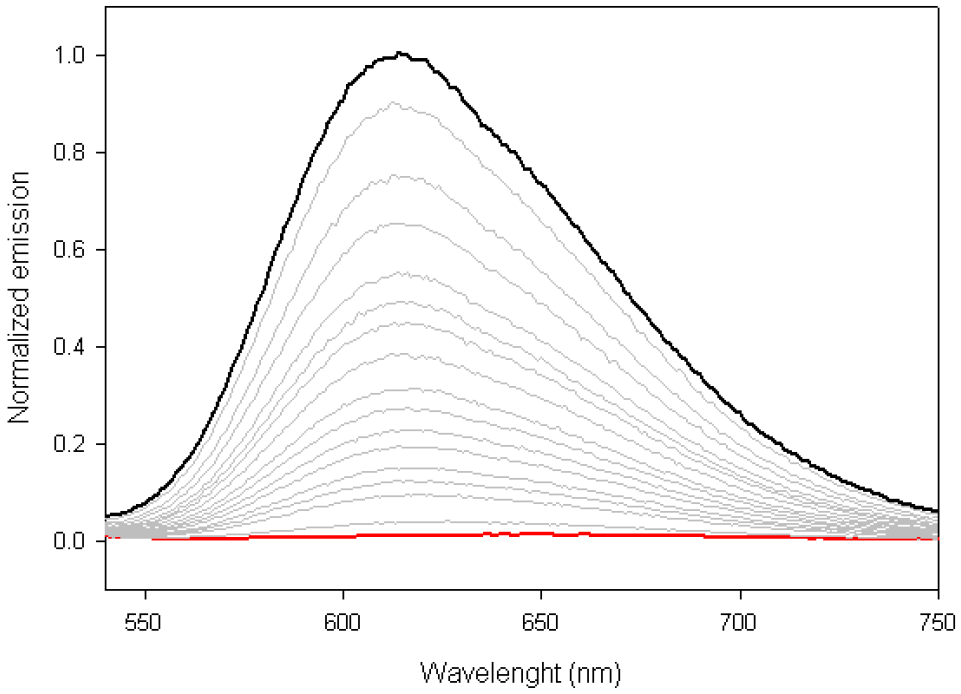

Figure S8. Top, luminescence spectra of a 2.0 μM solution of ***[Ru(dppz)]-R$_8$*** *in phosphate buffer (100 mM), KCl (1.0 M), pH 7.5 and evolution upon addition of aliquots of MYC oligonucleotide solution until saturation.*

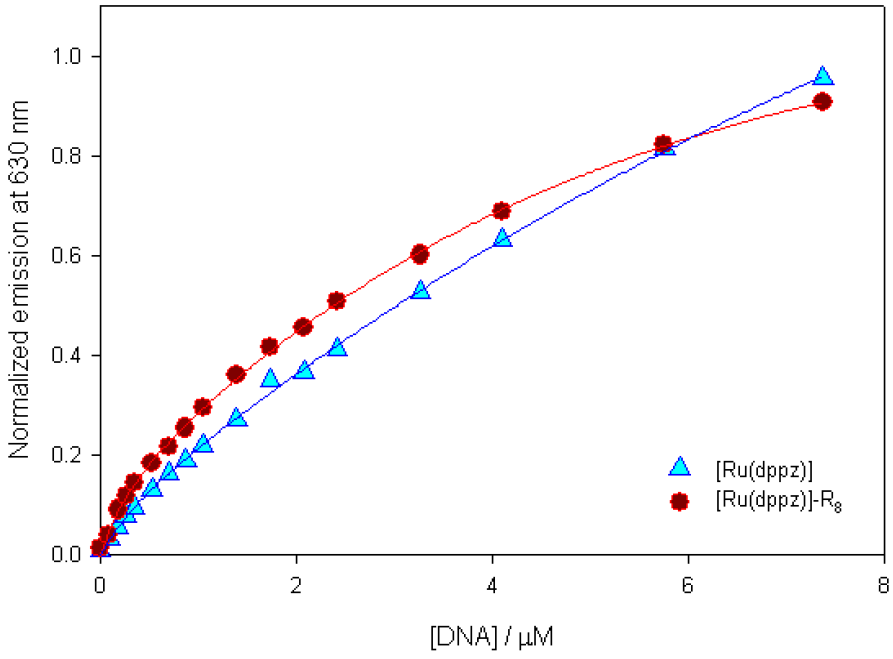

Figure S9. Profile of the titration experiments of ***[Ru(dppz)]*** *(cyan triangles) and* ***[Ru(dppz)]-R$_8$*** *(red circles) with MYC oligonucleotide at λ_{em} = 630 nm (emission intensity vs. concentration of DNA in the media) with the corresponding best fits.*

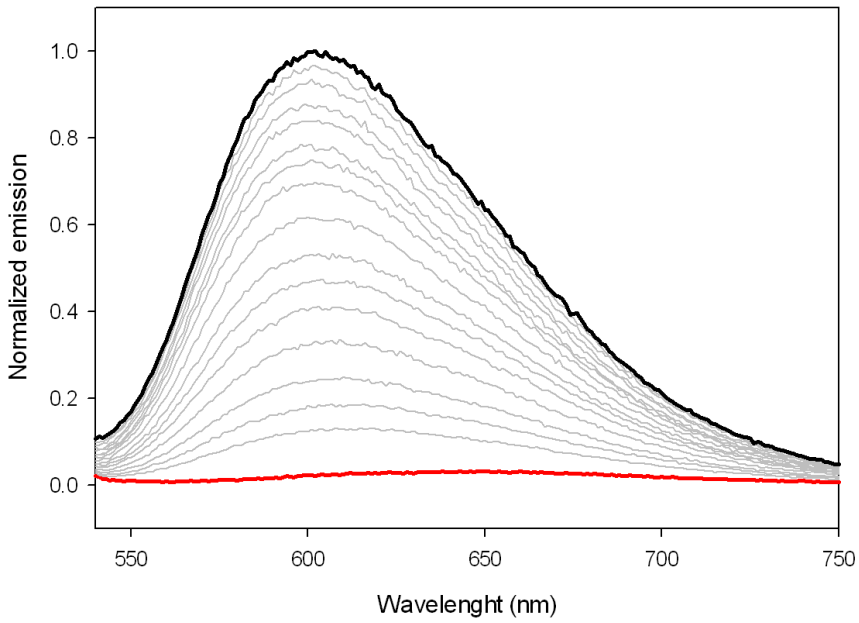

Figure S10. Top, luminescence spectra of a 2.0 μM solution of ***[Ru(dppz)$_2$]*** *in phosphate buffer (100 mM), KCl (1.0 M), pH 7.5 and evolution upon addition of aliquots of TEL oligonucleotide solution until saturation.*

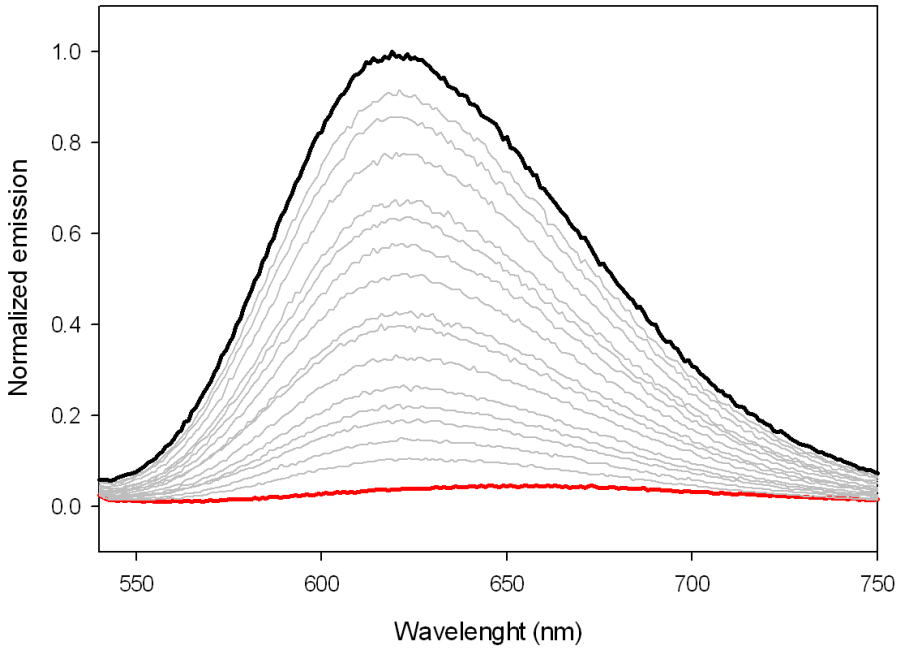

Figure S11. Top, luminescence spectra of a 2.0 μM solution of ***[Ru(dppz)$_2$]*** *in phosphate buffer (100 mM), KCl (1.0 M), pH 7.5 and evolution upon addition of aliquots of KIT oligonucleotide solution until saturation.*

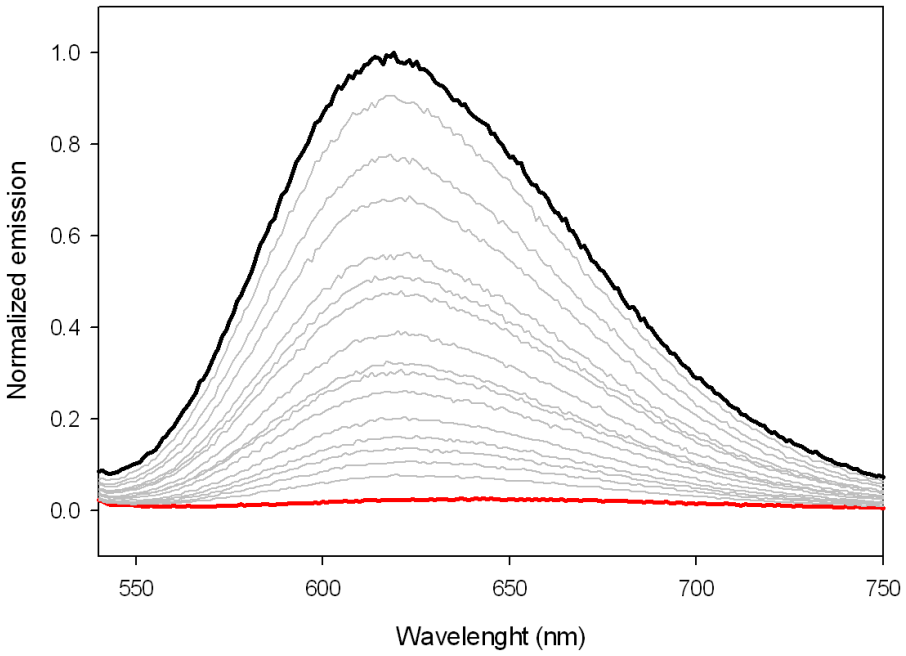

Figure S12. Top, luminescence spectra of a 2.0 μM solution of ***[Ru(dppz)$_2$]*** *in phosphate buffer (100 mM), KCl (1.0 M), pH 7.5 and evolution upon addition of aliquots of MYC oligonucleotide solution until saturation.*

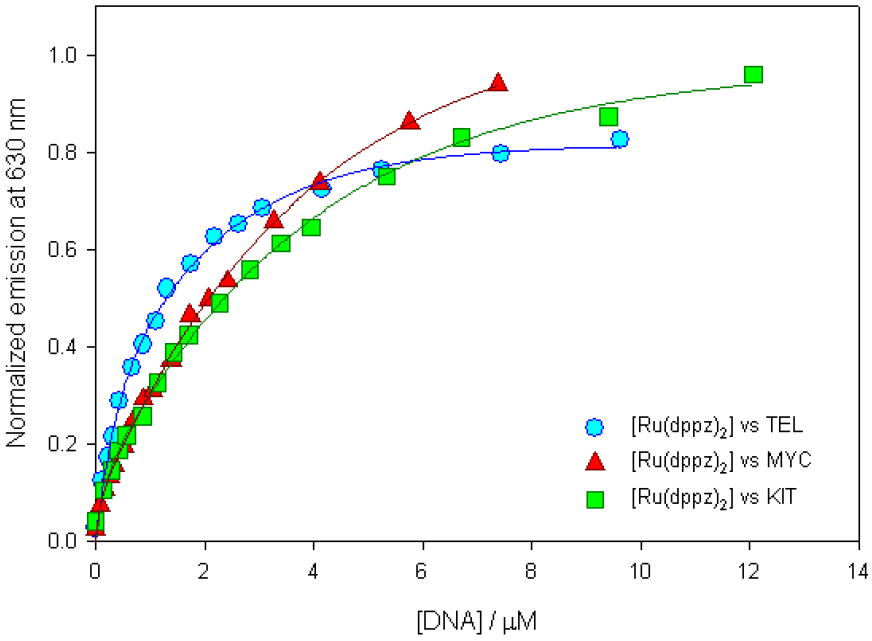

Figure S13. Profile of the titration experiments of ***[Ru(dppz)$_2$]*** *with TEL (cyan circles), c-MYC (red triangles) and c-KIT (green squares) oligonucleotides at λ_{em} = 630 nm (emission intensity vs. concentration of DNA in the media) with the corresponding best fits (red, green and black lines, respectively*).

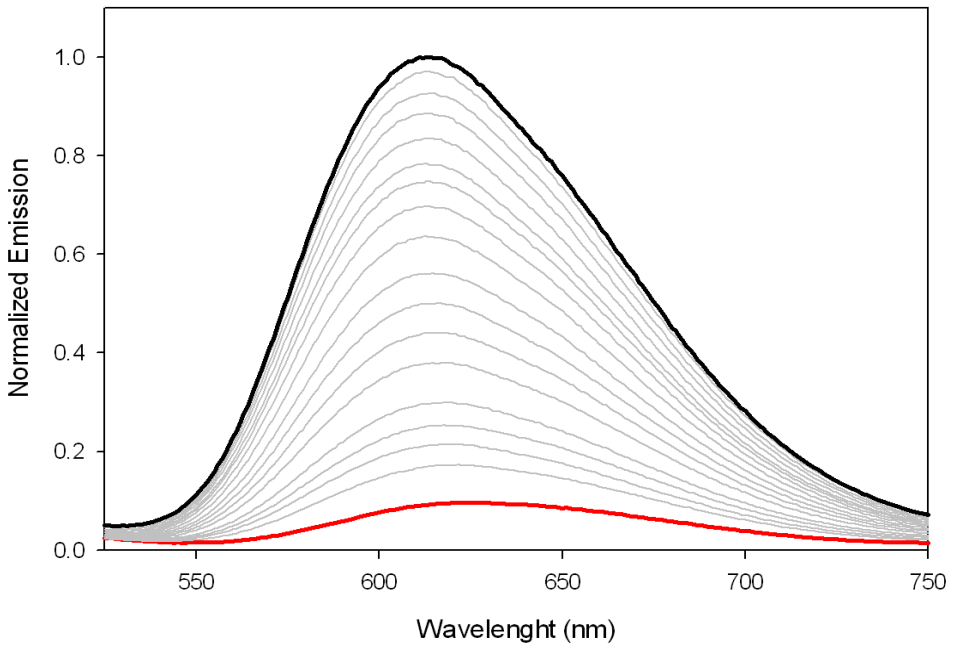

Figure S14. Top, luminescence spectra of a 2.0 μM solution of ***[Ru(dppz)$_2$]-R$_8$*** *in phosphate buffer (100 mM), KCl (1.0 M), pH 7.5 and evolution upon addition of aliquots of TEL oligonucleotide solution until saturation.*

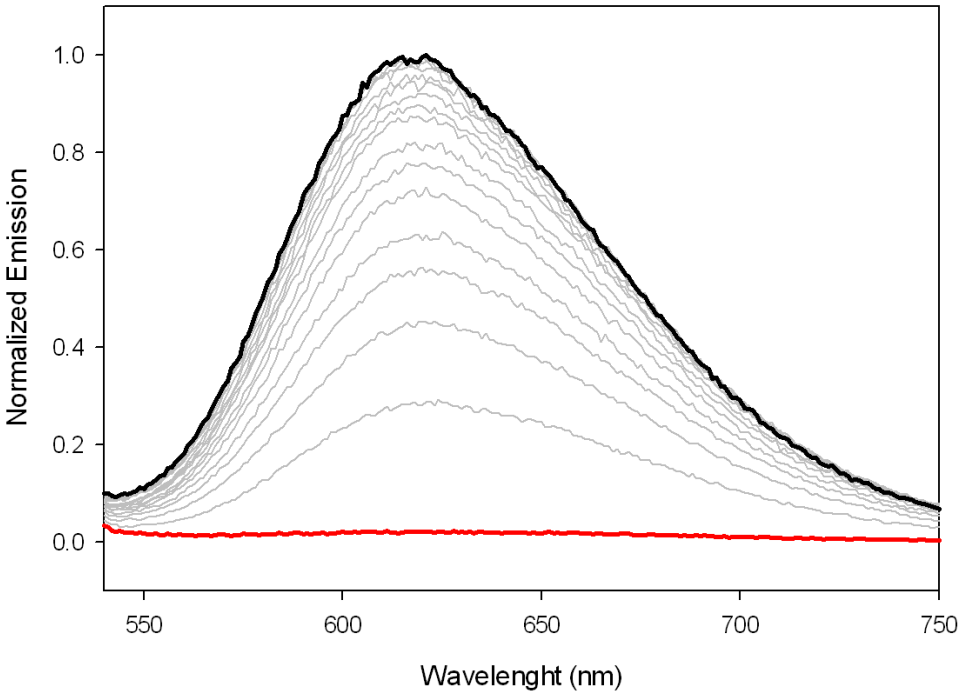

Figure S15. Top, luminescence spectra of a 2.0 μM solution of ***[Ru(dppz)$_2$]-R$_8$*** *in phosphate buffer (100 mM), KCl (1.0 M), pH 7.5 and evolution upon addition of aliquots of KIT oligonucleotide solution until saturation.*

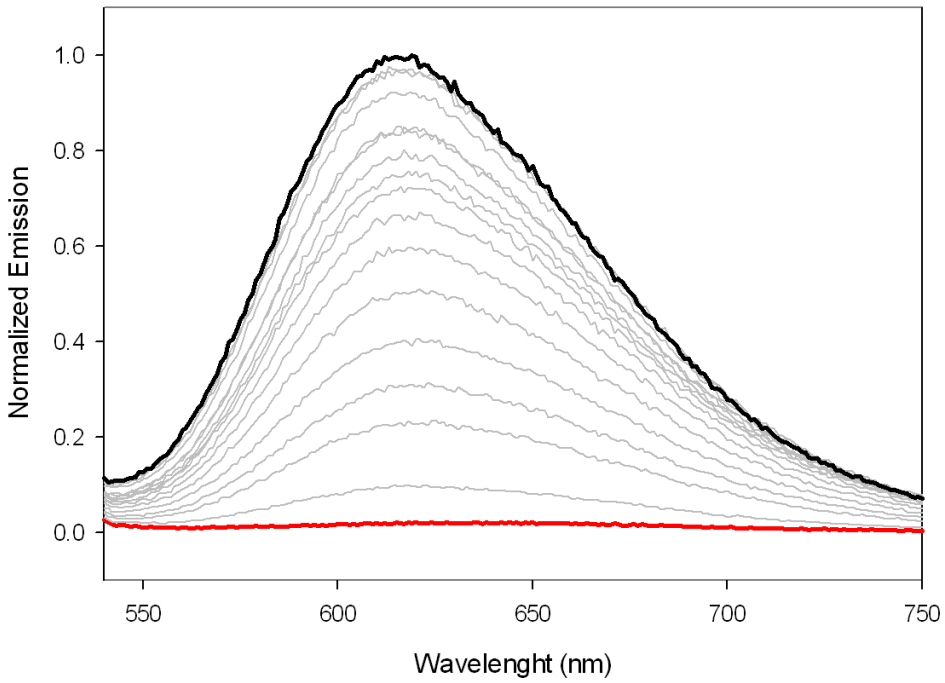

Figure S16. Top, luminescence spectra of a 2.0 μM solution of ***[Ru(dppz)$_2$]-R$_8$*** *in phosphate buffer (100 mM), KCl (1.0 M), pH 7.5 and evolution upon addition of aliquots of MYC oligonucleotide solution until saturation.*

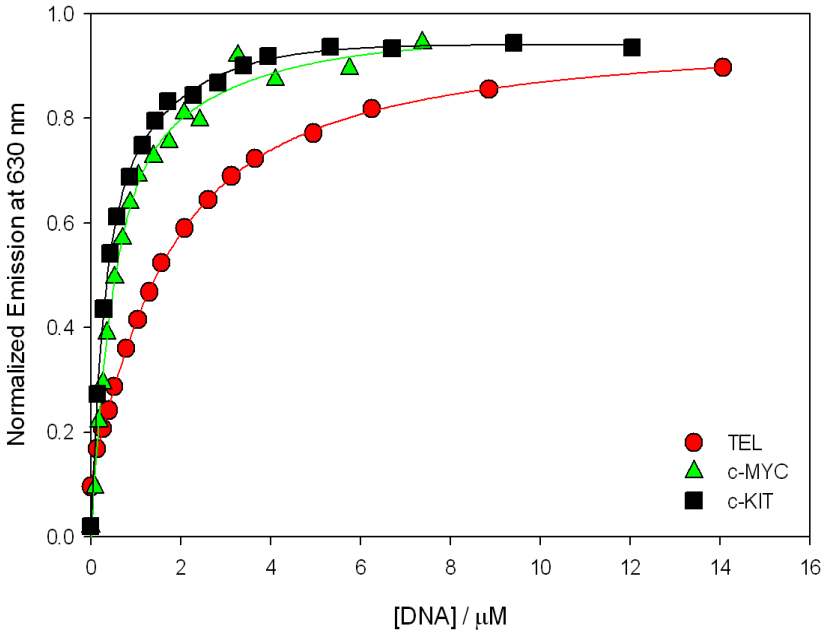

Figure S17. Profile of the titration experiments of ***[Ru(dppz)$_2$]-R$_8$*** *with TEL (red circles), c-MYC (green triangles) and c-KIT (black squares) oligonucleotides at λ_{em} = 630 nm (emission intensity vs. concentration of DNA in the media) with the corresponding best fits (red, green and black lines, respectively*).

Table S1. B-DNA and G-quadruplex sequences studied

Code	Complete Sequence (5'-3')
GAATTC	GGCGAATTCAGCTTTTTGCTGAATTCGCC
TEL	TAGGGTTAGGGTTAGGGTTAGGGTT
c-MYC	TTGAGGGTGGGTAGGGTGGGTAAA
c-KIT	TAGGGAGGGCGCTGGGAGGAGGGTT

UV-vis studies

To a solution of the selected Ru(II) metallopeptide (**[Ru(dppz)]** and **[Ru(dppz)]-R_8**) in phosphate buffer (10 mM), pH 7.5 and KCl (100 mM), an aliquot of G-quadruplex (*TEL*, *c-MYC* or *c-KIT*) stock solution (in water) was added in order to reach a [Ru]/[DNA] ratio of 0.5. The absorption spectra of **[Ru(dppz)]** and **[Ru(dppz)]-R_8** were recorded before and after the addition of the corresponding oligonucleotide. The sequences of the oligonucleotides studied are listed in Table S1.

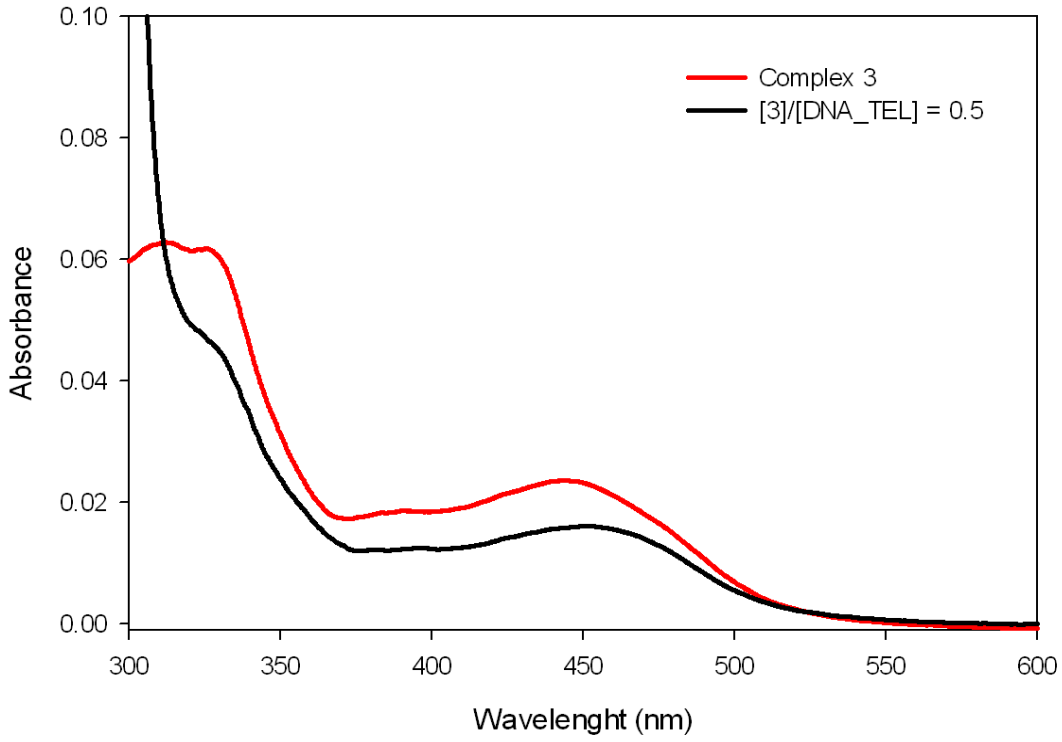

*Figure S18. UV-vis absorption spectra of metallopeptide **[Ru(dppz)]** (4.0 μM) before (red line) and after (black line) the addition of a solution of TEL oligonucleotide.*

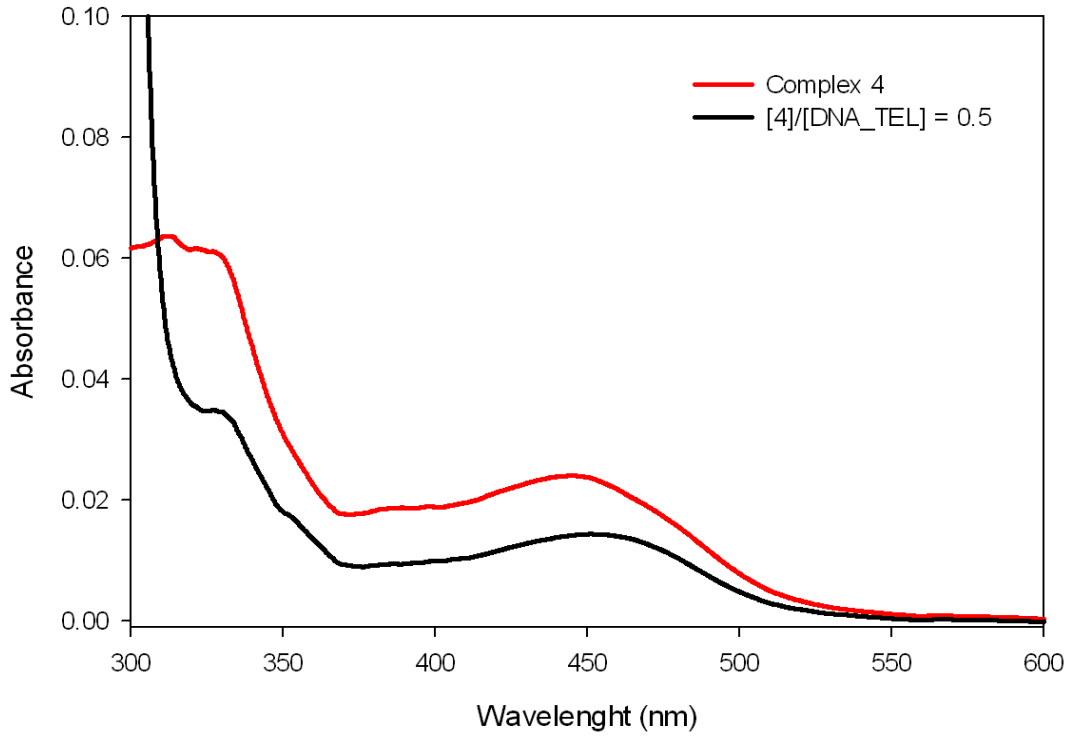

Figure S19. UV-vis absorption spectra of metallopeptide ***[Ru(dppz)]-R$_8$*** *(4.1 μM) before (red line) and after (black line) the addition of a solution of TEL oligonucleotide.*

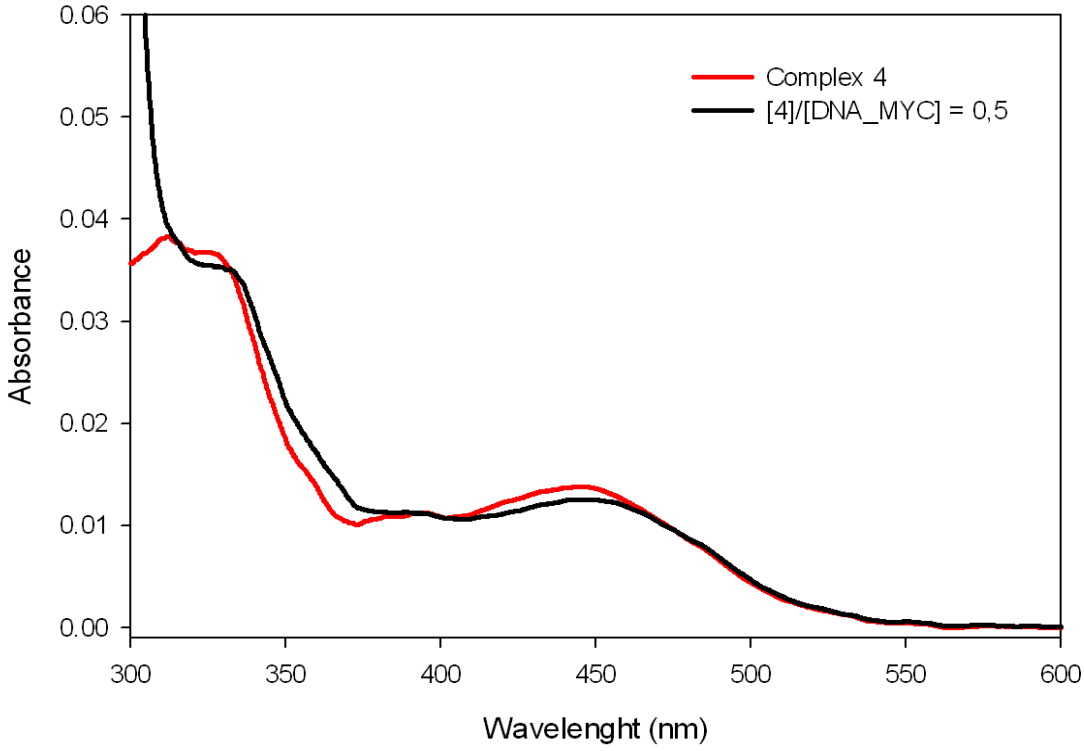

Figure S20. UV-vis absorption spectra of metallopeptide ***[Ru(dppz)]-R$_8$*** *(2.3 μM) before (red line) and after (black line) the addition of a solution of c-MYC oligonucleotide.*

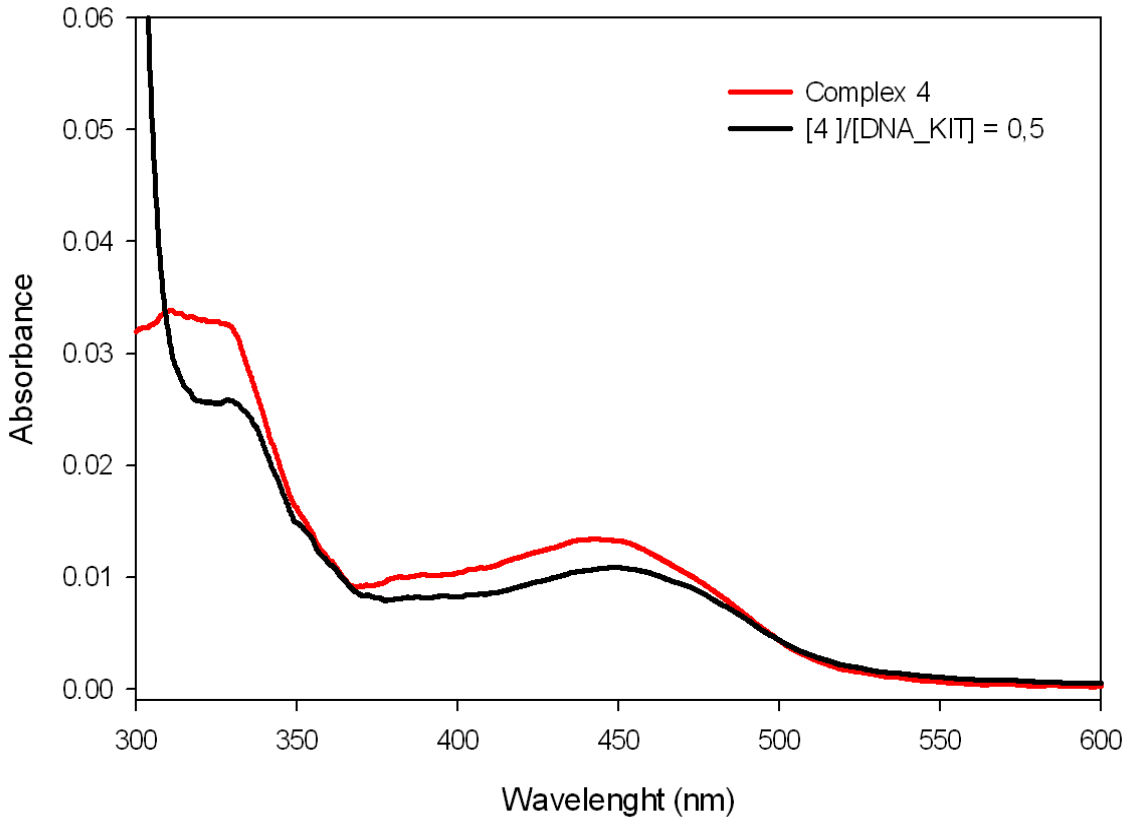

Figure S21. UV-vis absorption spectra of metallopeptide ***[Ru(dppz)]-R$_8$*** *(2.2 μM) before (red line) and after (black line) the addition of a solution of c-KIT oligonucleotide.*

CD studies

To a solution of the selected G-quadruplex oligonucleotide (*TEL*, *c-MYC* and *c-KIT*) in phosphate buffer (10 mM), pH 7.5 and KCl (100 mM), an aliquot of a Ru(II) metallopeptide (**[Ru(dppz)]** and **[Ru(dppz)]-R_8**) in water was added in order to reach a [Ru]/[DNA] ratio of 0.2. The CD spectrum of the selected G-quadruplex oligonucleotide was recorded before and after the addition of the corresponding metallopeptide. The studied oligonucleotides are listed in Table S1.

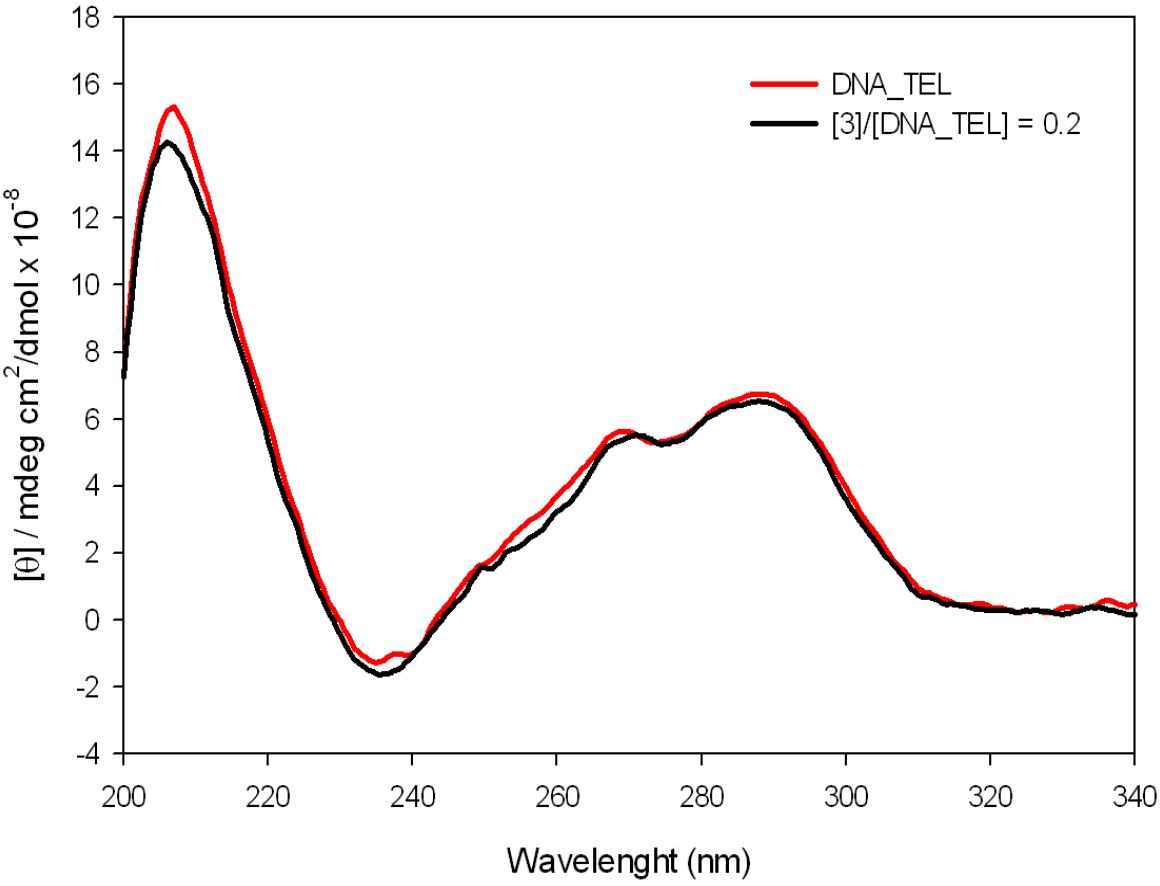

Figure S22. CD spectra of TEL oligonucleotide (10.0 μM) before (red line) and after (black line) the addition of a solution of metallopeptide ***[Ru(dppz)]****.*

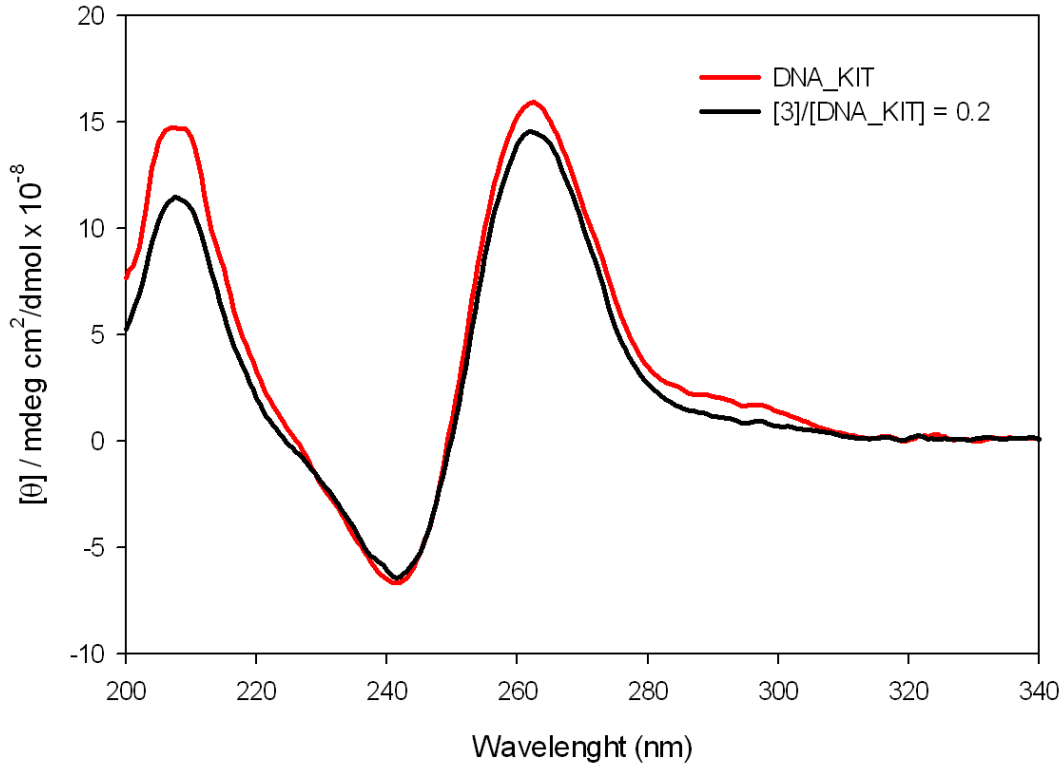

Figure S23. CD spectra of c-KIT oligonucleotide (10.0 μM) before (red line) and after (black line) the addition of a solution of metallopeptide ***[Ru(dppz)]****.*

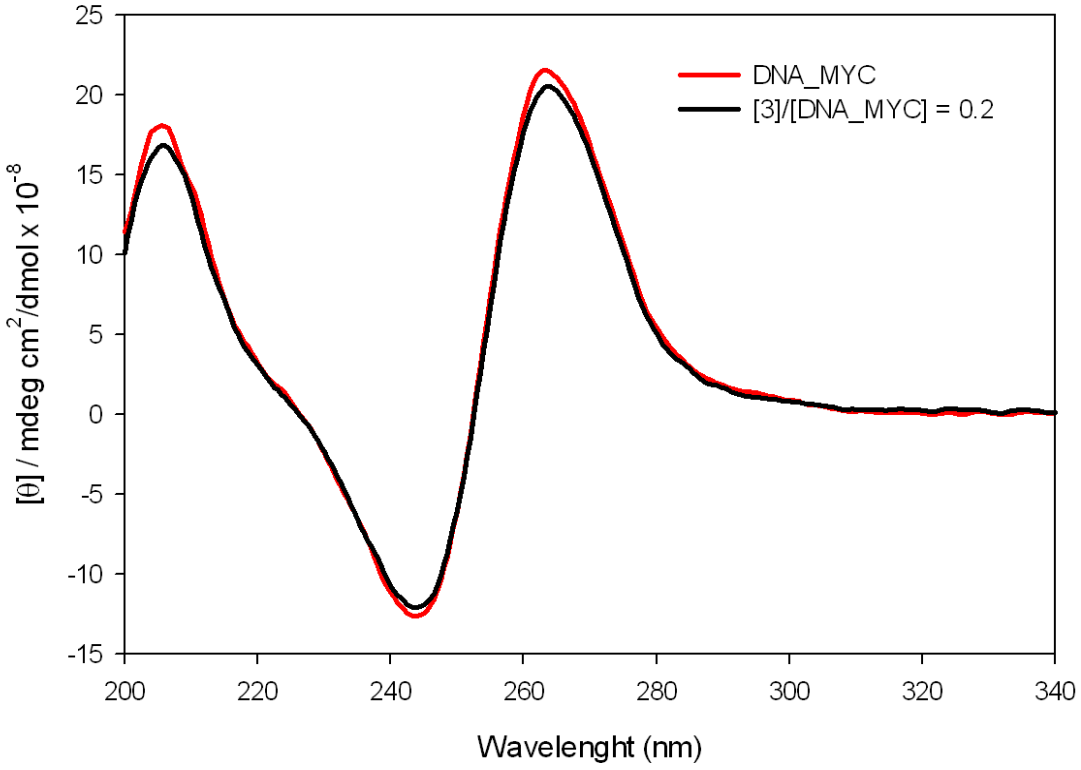

Figure S24. CD spectra of c-MYC oligonucleotide (10.0 μM) before (red line) and after (black line) the addition of a solution of metallopeptide ***[Ru(dppz)]****.*

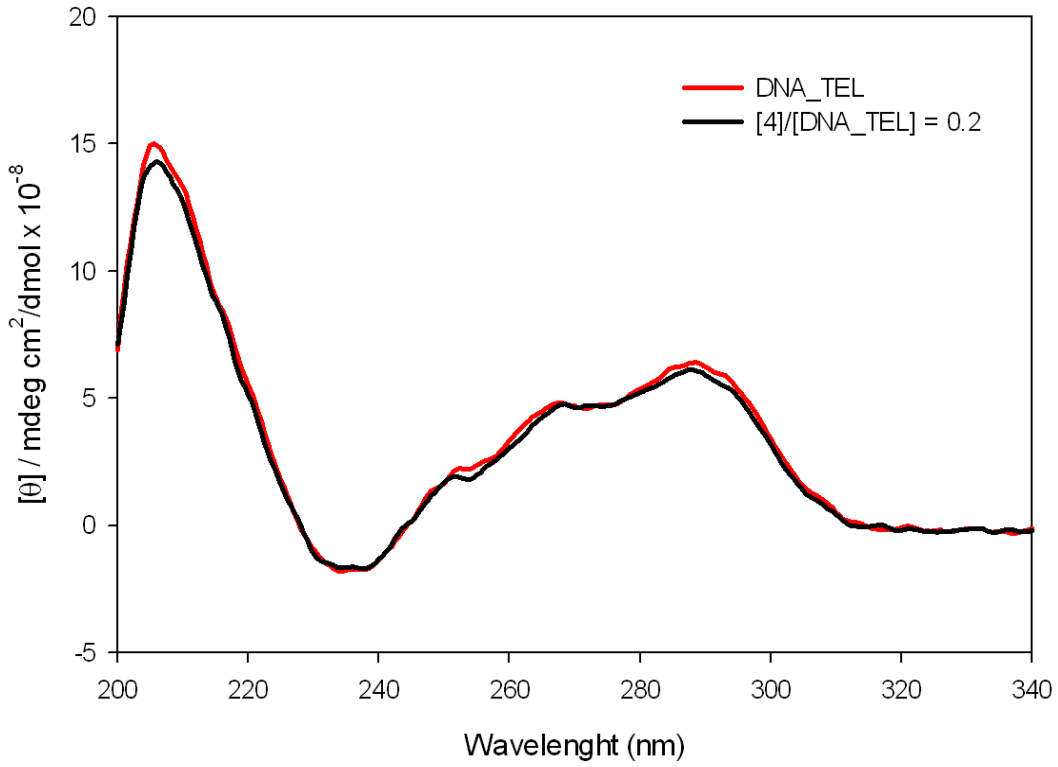

Figure S25. CD spectra of TEL oligonucleotide (10.0 μM) before (red line) and after (black line) the addition of a solution of metallopeptide ***[Ru(dppz)]-R$_8$***.

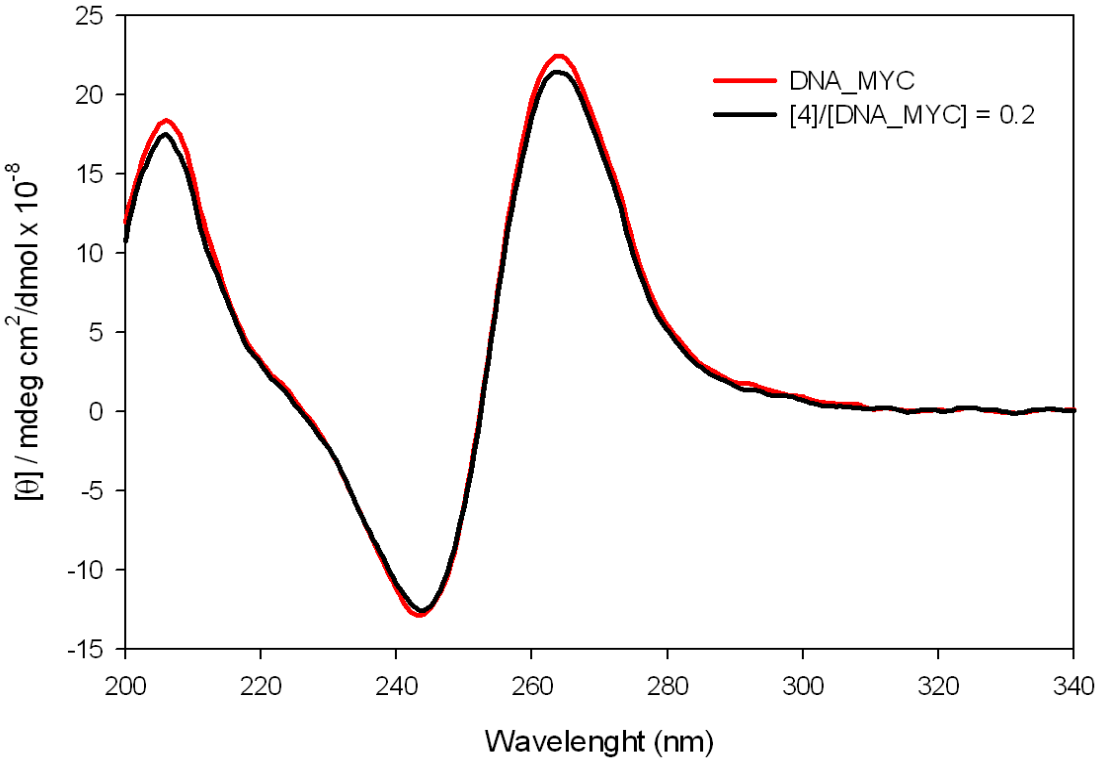

Figure S26. CD spectra of c-MYC oligonucleotide (10.0 μM) before (red line) and after (black line) the addition of a solution of metallopeptide ***[Ru(dppz)]-R$_8$***.

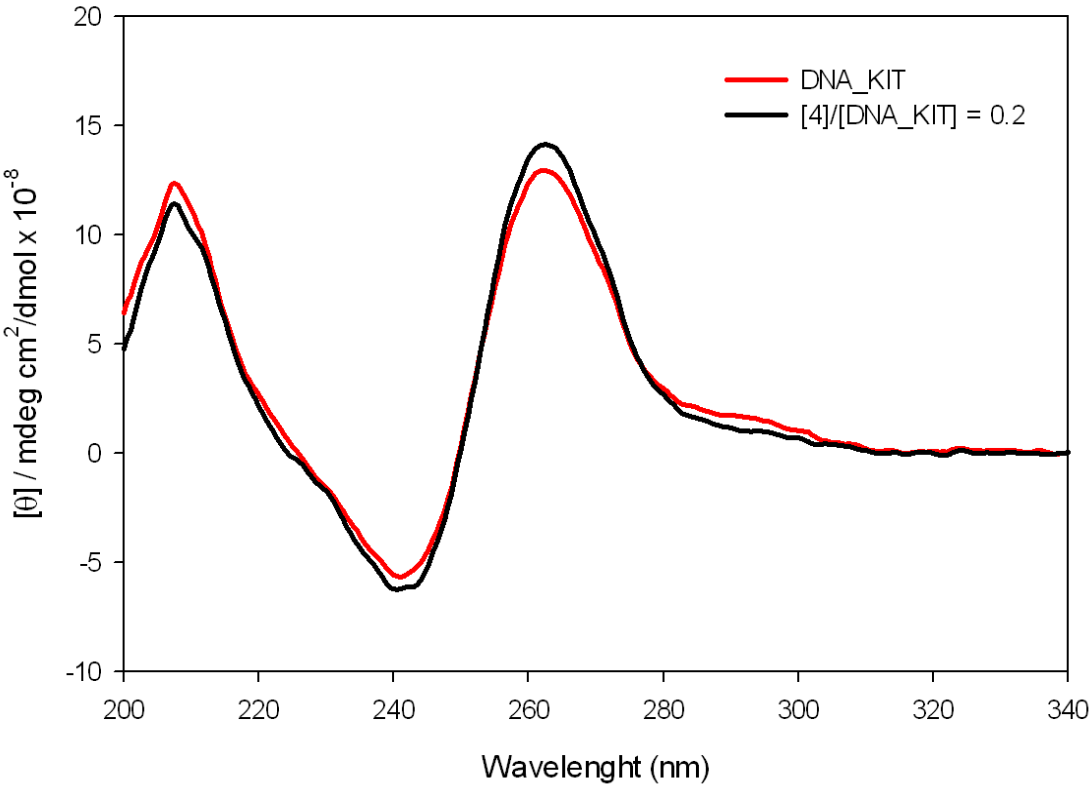

Figure S27. CD spectra of c-KIT oligonucleotide (10.0 μM) before (red line) and after (black line) the addition of a solution of metallopeptide ***[Ru(dppz)]-R$_8$***.

Docking studies

Docking calculations were performed with *AutoDock 4.2* with the Lamarckian genetic algorithm.[5] Molecular geometries for the ligands and atomic charges were computed with *MOPAC16* at the PM6-d3h4 level within a continuum model of water in the singlet ground state.[6] Results were analyzed and/or rendered with *AutoDockTools*, *Pymol* [7] and *Chimera*.[8]

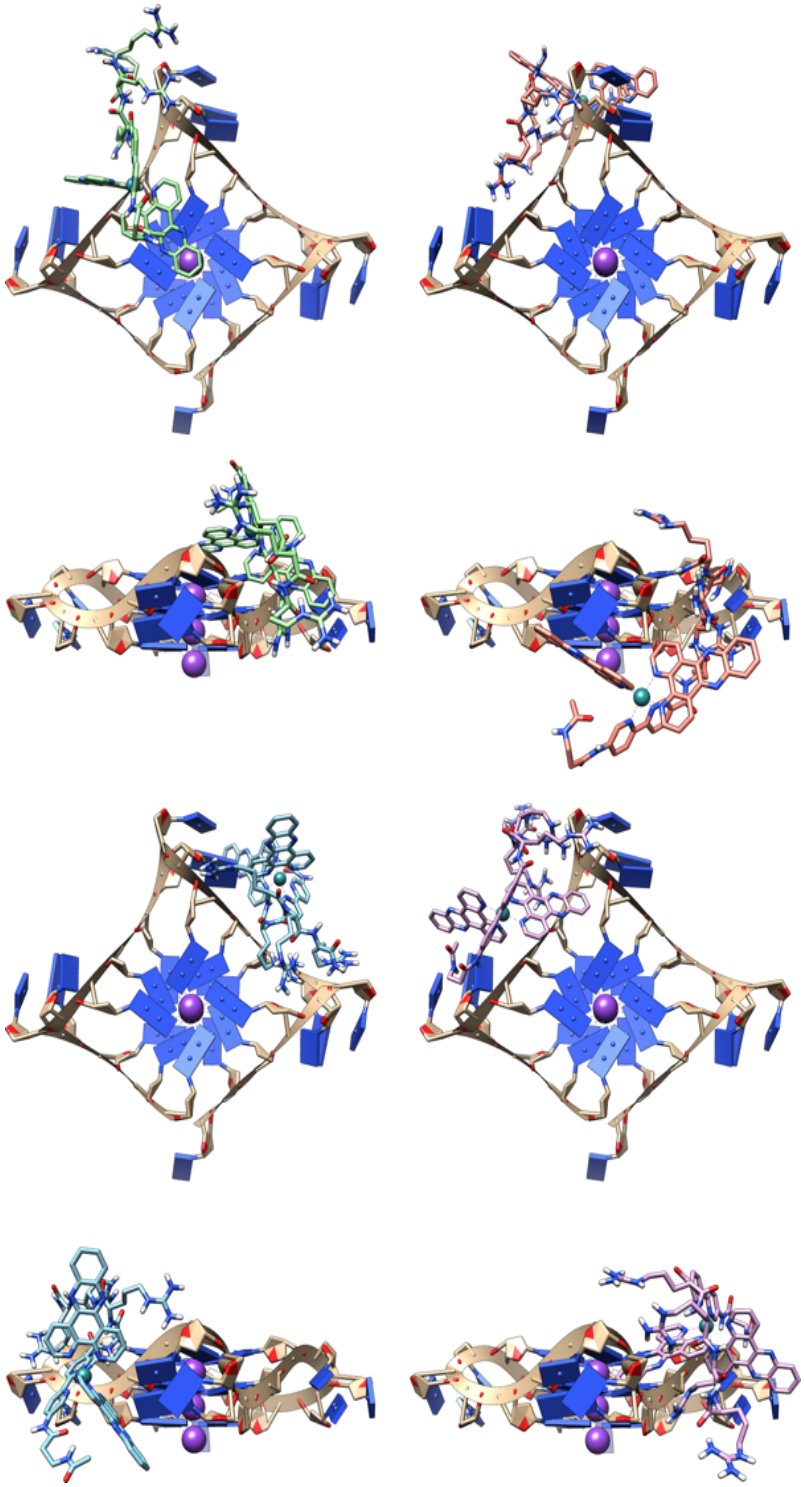

Figure S28. Best docking poses (lowest energy) of the four ***[Ru(dppz)$_2$]-R$_4$*** *stereoisomers to the TEL (1kf1) quadruplex from two perspectives. Top, two lambda stereoisomers, bottom two delta stereoisomers. Violet and green spheres represent the potassium and ruthenium atoms respectively.*

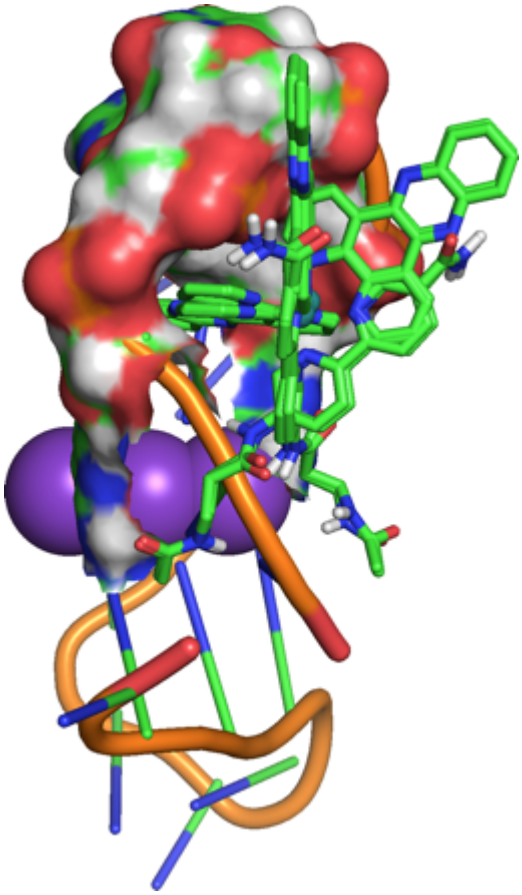

Figure S29. Best docking pose (lowest energy) of ***[Ru(dppz)$_2$]*** *to the TEL (1kf1) quadruplex. Violet and green spheres represent the potassium and ruthenium atoms respectively. Van der Waals surface highlights the pocket formed by the GTTAG sequence in the quadruplex.*

Fluorescent microscopy studies

Semi-confluent monolayers of African green monkey kidney epithelial (Vero) cells were grown on glass bottom 35 mm dishes in Dulbeccos modified Eagle Medium (DMEM) containing 10% of FBS (fetal bovine serum). This cell line was selected, as it is a standard mammalian culture cell similar to human and which looks very good under a microscope. For the assays, the cells were washed three times with DMEM containing no FBS or antibiotics, and incubated with 5 μM of the compound **[Ru(dppz)]-R_8** in DMEM without FBS during 24 hr, at 37 °C in a 5% CO_2 humidified atmosphere. Then, the cells were gently washed 5 times with phosphate buffered saline (PBS), and observed under the fluorescence microscope in DMEM without fixation. Alternatively, the cells were incubated for 30 minutes with 25 μM of the compounds **[Ru(dppz)]** and **[Ru(dppz)]-R_8** in DMEM without FBS during 30 minutes, at 37 °C in a 5% CO_2 humidified atmosphere. After that, the cells were washed 5 times with phosphate buffered saline (PBS), fresh DMEM was added and the cells were continuously monitored for four hours under the fluorescence microscope in DMEM without fixation. All images were obtained with a *Zyla 4.2* camera (*Andor*) mounted on a *NIKON Ti E* inverted microscope equipped with incubation chamber. Images were manipulated with *NIS* software (Nikon) and *Adobe Photoshop*.

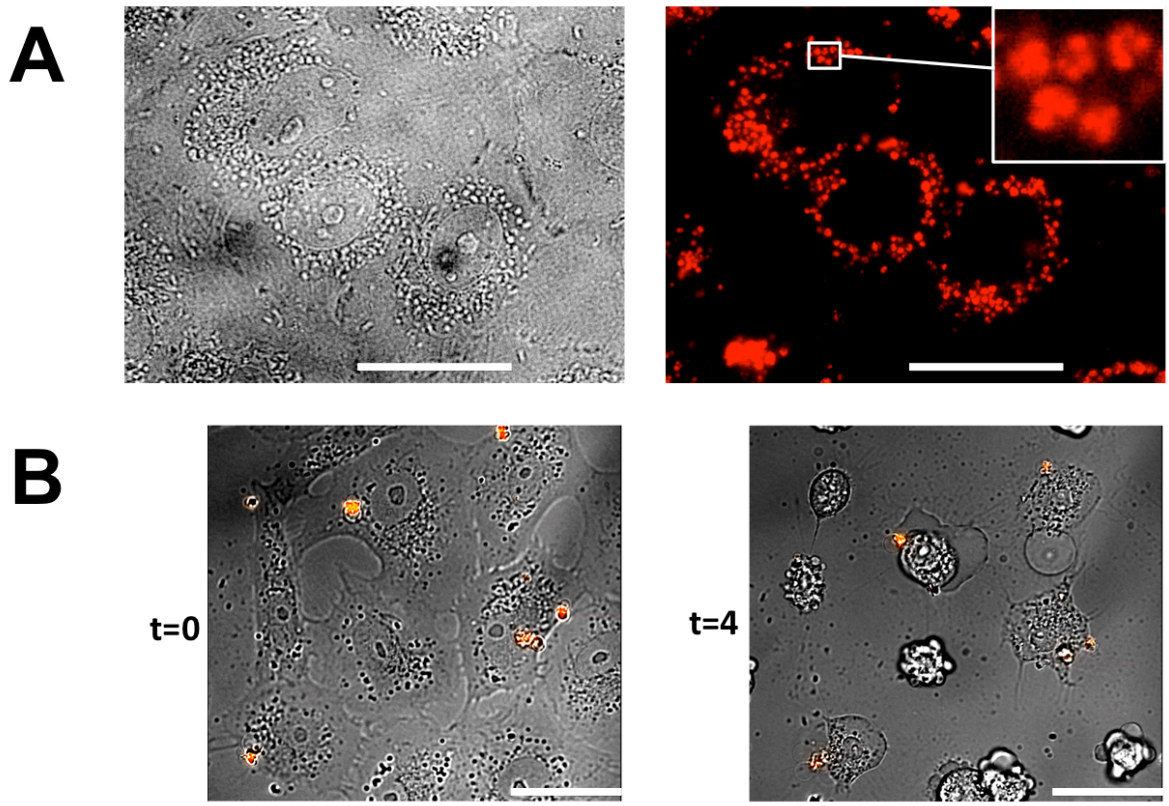

Figure S30. A) Vero cells monolayers incubated with 5 μM solution of ***[Ru(dppz)]-R_8*** *in medium DMEM without serum for 24 h. Bright field (left) and red-emission fluorescence micrographies (right) were taken from unfixed living cells at 1000X magnification. The scale bar corresponds to 20 μm. B) Monolayers of Vero cells incubated with 25 μM of* ***[Ru(dppz)]-R_8*** *in DMEM without serum for 30 min, followed by washing three times with PBS, and further incubated at 37 °C in DMEM without serum. The figure shows snapshots at the starting incubation time (t = 0) and after 4 h of incubation (t = 4h) of a time-lapse video (see ESI†, video_1) showing merged bright field and fluorescence images. As in A, the scale bar corresponds to 20 μm*

Finally, we performed cell internalization studies. In particular, we incubated Vero cell monolayers with the metallopeptide **[Ru(dppz)]-R_8** at 5 μM for 24 h. Upon observation under the fluorescence microscope, we observed a punctate fluorescent pattern in the cell cytoplasm, consistent with endocytic internalization (Figure S16A). The irregular staining of some of the observed vesicles (see inlay in Figure S16A) suggests that at least part of the compound is aggregating inside the endocytic vesicles. Such effect might be due to an elevated intra-vesicle concentration of the metallopeptide. It is noteworthy that all the cells in the culture appear live and healthy, even after 24 h of incubation with the metallopeptide at this concentration.

In a different experiment, Vero cells were incubated with a higher concentration of **[Ru(dppz)]-R_8** (25 μM) for 30 min. The cells were then washed three times with PBS before replacing the medium with fresh DMEM without serum. The fluorescence emission of the metallopeptide was continuously recorded together with bright field monitoring of the culture at 37 °C for 4 h after the addition of the compound (Figure S16B; see ESI: video_1). Interestingly, at high concentration the metallopeptide forms non-uniform aggregates over the cells that cause the disruption of the plasmatic membrane, and leakage of the cytosol content. Furthermore, the remaining cells not associated with an aggregate die within the four hours showing typical signs of apoptosis. Those results suggest that, as previously reported for other octaarginine derivatives, the metallopeptide is directly internalized at high concentration, thus causing apoptosis of the cells, while preventing its intracellular accumulation to a detectable level. Further investigation is needed to clarify this issue. Importantly, control experiments demonstrated that the complex [Ru(dppz)] lacking the octaarginine domain does not show cytotoxic or internalization properties (Figure S17).

Video 1: Monolayers of Vero cells were incubated with 25 μM of **[Ru(dppz)]-R_8** in DMEM without serum for 30 minutes. After that, the medium was removed, the cells washed three times with PBS, and further incubated at 37 ºC in DMEM without serum. The time-lapse video shows 5min. lapsed captures from the starting incubation time until 4,5 hours of incubation. A scale bar and the acquisition time are shown superimposed.

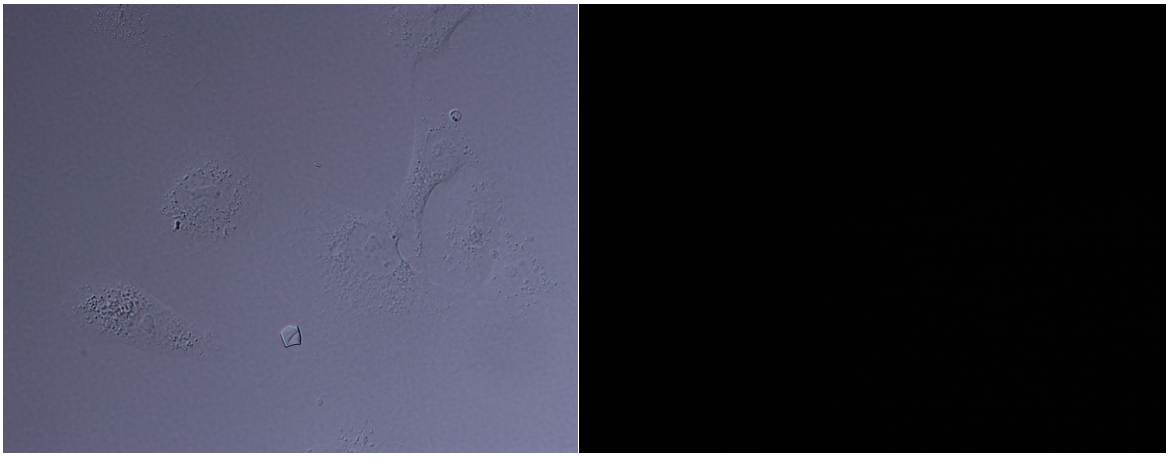

*Figure S31. Monolayers of Vero cells were incubated with 25 μM of **[Ru(dppz)]** in DMEM without serum for 30 minutes. After that, the medium was removed, the cells washed three times with PBS, and further incubated at 37ºC in DMEM without serum. Brightfield (left) and red-emission fluorescence pictures (right) were taken from unfixed living cells at 1000X magnification.*

References

[1] I. Gamba, I. Salvadó, G. Rama, M. Bertazzon, M. I. Sánchez, V. Sánchez-Pedregal, J. Martínez-Costas, R. F. Brissos, P. Gámez, J. L. Mascareñas, M. Vázquez López, M. E. Vázquez, *Chem. Eur. J.*, **2013**, *19*, 13369.

[2] P. Evans, A. Spencer, G. Wilkinson, *J. C. S. Dalton*, **1973**, 204.

[3] J. E. Dickenson, L. A. Summers, *Aust. J. Chem*., **1970**, *23*, 1023.

[4] S. Shi, X. Geng, J. Zhao, T. Yao, C. Wang, D. Yang, L. Zheng, L. Ji, *Biochimie*, **2010**, *92*, 370.

[5] G. M. Morris, R. Huey, W. Lindstrom, M. F. Sanner, R. K. Belew, D. S. Goodsell, A. J. Olson, *Autodock4 and AutoDockTools4: automated docking with selective receptor flexibility. J. Computational Chemistry,* **2009**, *16*, 2785.

[6] J. J. P. Stewart, MOPAC2016, Stewart Computational Chemistry, Colorado Springs, CO, 2016, http://OpenMOPAC.net (February 8, 2016).

[7] *The PyMOL Molecular Graphics System*, Version 1.7, Schrödinger, LLC.

[8] *UCSF Chimera--a visualization system for exploratory research and analysis.* E. F. Pettersen, T. D. Goddard, C. C. Huang, G. S. Couch, D. M. Greenblatt, E. C. Meng, T. E. Ferrin, *J Comput Chem.,* **2004**, *25*, 1605.